UNIVERSITY OF IOANNINA
SCHOOL OF SCIENCES
DEPARTMENT OF MATHEMATICS
APPLIED MATHEMATICS
AND ENGINEERING RESEARCH

The Finite Element Method in Fluid Mechanics: Theoretical and Applied Approaches

Konstantina Kyriakoudi

MASTER THESIS

Ioannina, 2019

ΠΑΝΕΠΙΣΤΗΜΙΟ ΙΩΑΝΝΙΝΩΝ
ΣΧΟΛΗ ΘΕΤΙΚΩΝ ΕΠΙΣΤΗΜΩΝ
ΤΜΗΜΑ ΜΑΘΗΜΑΤΙΚΩΝ
ΤΟΜΕΑΣ ΕΦΑΡΜΟΣΜΕΝΩΝ ΜΑΘΗΜΑΤΙΚΩΝ
ΚΑΙ ΜΗΧΑΝΙΚΗΣ ΕΡΕΥΝΑΣ

Η Μεθοδος των Πεπερασμενων Στοιχειων στη Μηχανικη των Ρευστων: Θεωρια και Εφαρμογες

Κωνσταντίνα Κυριακούδη

ΜΕΤΑΠΤΥΧΙΑΚΗ ΔΙΑΤΡΙΒΗ

Ιωάννινα, 2019

Αφιερώνεται στους γονείς μου Χρήστο και Κατερίνα, στον αδερφό μου Δημήτρη, στον παππού Κωνσταντίνο και τη γιαγιά Λαμπρινή και στον Βασίλη.

Dedicated to my parents Christos and Katerina, to my brother Dimitris, to my grandparents Konstantinos and Lamprini and to Vassilis.

Η παρούσα Μεταπτυχιακή Διατριβή εκπονήθηκε στο πλαίσιο των σπουδών για την απόκτηση του Μεταπτυχιακού Διπλώματος Ειδίκευσης στα Εφαρμοσμένα Μαθηματικά και Πληροφορική που απονέμει το Τμήμα Μαθηματικών του Πανεπιστημίου Ιωαννίνων.

Εγκρίθηκε την 27/06/2019 από την εξεταστική επιτροπή:

Ονοματεπώνυμο	**Βαθμίδα**
Μιχαήλ Ξένος	Αναπληρωτής Καθηγητής (Επιβλέπων)
Δημήτριος Νούτσος	Καθηγητής
Ευγενία Πετροπούλου	Αναπληρώτρια Καθηγήτρια

ΥΠΕΥΘΥΝΗ ΔΗΛΩΣΗ

"Δηλώνω υπεύθυνα ότι η παρούσα διατριβή εκπονήθηκε κάτω από τους διεθνείς ηθικούς και ακαδημαϊκούς κανόνες δεοντολογίας και προστασίας της πνευματικής ιδιοκτησίας. Σύμφωνα με τους κανόνες αυτούς, δεν έχω προβεί σε ιδιοποίηση ξένου επιστημονικού έργου και έχω πλήρως αναφέρει τις πηγές που χρησιμοποίησα στην εργασία αυτή."

Κωνσταντίνα Κυριακούδη

Ευχαριστιες

Η παρούσα διατριβή έχει πραγματοποιηθεί στο Τμήμα Μαθηματικών του Πανεπιστημίου Ιωαννίνων. Με την ολοκλήρωση της παρούσας διατριβής θα ήθελα να ευχαριστήσω κάποιους ανθρώπους, των οποίων η συμβολή ήταν καθοριστική σε αυτή τη μελέτη.

Αρχικά θα ήθελα να ευχαριστήσω τον επιβλέποντα καθηγητή μου κ. Μιχαήλ Ξένο, για τη βοήθεια, τις πολύτιμες συμβουλές, τον χρόνο, την υποστήριξη, την καθοδήγηση, την ενθάρρυνση και αμέριστη συμπαράσταση που μου προσέφερε κατά τη διάρκεια της εκπόνησης της εργασίας.Ελπίζω ότι και ο ίδιος γνωρίζει ότι τον εκτιμώ όχι μόνο ως καθηγητή, αλλά και ως άνθρωπο.

Ιδιαίτερα θέλω να ευχαριστήσω και τα άλλα δύο μέλη της τριμελούς επιτροπής, κ. Δημήτριο Νούτσο και την κα. Ευγενία Πετροπούλου για το ενδιαφέρον που έδειξαν, τον χρόνο που διέθεσαν αλλά και για τις εύστοχες παρατηρήσεις και υποδείξεις τους στην διατριβή αυτή με σκοπό την βελτίωση της.

Ακόμη θα ήθελα να ευχαριστήσω όλους του διδάσκοντες του Τμήματος Μαθηματικών για τις γνώσεις που μου προσέφεραν σε Προπτυχιακό και Μεταπτυχιακό επίπεδο και τη συνεργασία που είχαμε όλα αυτά τα χρόνια.

Θα ήθελα, επιπλέον, να πω ένα ευχαριστώ στους Δρ. Αναστάσιο Ράπτη και κ. Alessandro Tonelli, οι οποίοι ήταν πάντα πρόθυμοι να βοηθήσουν και να μου εξηγήσουν πολλές από τις απορίες που προέκυπταν κατά τη διάρκεια εκπόνησης της διατριβής.

Το πιο μεγάλο ευχαριστώ από όλα τα παραπάνω ανήκει δικαιωματικά στους γονείς μου, που με στήριξαν με όλους τους δυνατούς τρόπους ώστε να ολοκληρώσω τις μεταπτυχιακές μου σπουδές και θα συνεχίσουν να με στηρίζουν σε όλα τα μελλοντικά μου σχέδια.

Ιωάννινα 2019,
Κωνσταντίνα Κυριακούδη

Acknowledgements

This dissertation has been compiled at the Department of Mathematics of the University of Ioannina. With the completion of this dissertation, I would like to thank some people, whose contribution was decisive in this study.

Initially, I would like to thank my supervisor, Dr. Michael Xenos, for his help, valuable advice, time, support, guidance and the encouragement that he offered me during my study. I hope that he knows that I appreciate him not only as a professor, but also as a person.

In particular, I would like to thank the other two members of the three-member committee, Prof. Dimitrios Noutsos and Prof. Eugenia Petropoulou for the interest they showed, the time they spent, but also for their precise corrections and suggestions in this dissertation for its improvement.

I would also like to thank all the professors of the Department of Mathematics for the knowledge they have offered me at the undergraduate and postgraduate level and the cooperation we have had over the years.

Furthermore, I would like to thank Dr. Anastasios Raptis and Mr. Alessandro Tonelli, who were always willing to help by explaining to me many of the questions that emerged during the dissertation.

The biggest thank you belongs rightfully to my parents, who supported me in every possible way to complete my graduate studies and will continue to support me in all my future plans.

Ioannina 2019,
Konstantina Kyriakoudi

Περιληψη

Η μέθοδος πεπερασμένων στοιχείων είναι μια αριθμητική μέθοδος για τον υπολογισμό προσεγγιστικών λύσεων μερικών διαφορικών εξισώσεων. Η μέθοδος αυτή αποτελεί ισχυρό εργαλείο στη μελέτη διάφορων προβλημάτων και βρίσκει μεγάλο αριθμό εφαρμογών. Εμείς εδώ θα επικεντρωθούμε στην εφαρμογή της μεθόδου σε προβλήματα Ρευστομηχανικής. Η Ρευστομηχανική αποτελεί ιδιαίτερο κλάδο της κλασικής μηχανικής με κύριο αντικείμενο έρευνας και μελέτης τη στατική και δυναμική συμπεριφορά των ρευστών. Ως ρευστό χαρακτηρίζεται οποιαδήποτε ουσία παρουσιάζει ροή δηλαδή αναφέρεται σε υγρά και αέρια των οποίων οι δυνάμεις συνοχής είναι ασθενείς, έτσι ώστε να λαμβάνουν κάθε φορά το σχήμα του χώρου που καταλαμβάνουν ή του μέσου δια του οποίου κινούνται.

Στην παρούσα εργασία θα επιχειρήσουμε να επιλύσουμε τις μερικές διαφορικές εξισώσεις που περιγράφουν την κίνηση των ρευστών. Επειδή όμως η λύση των εξισώσεων αυτών δεν είναι πάντα εφικτή, όπως στην περίτωση των εξισώσεων Navier–Stokes, είναι αναγκαίο να επεκταθούμε σε νεόυς τρόπους επίλυσης αυτών, όπως την μέθοδο των Πεπερασμένων Στοιχείων. Αρχικά θα παρουσιάσουμε την μέθοδο μαζί με τα βασικά θεωρήματα ύπαρξης και μοναδικότητας των λύσεων που προκύπτουν.

Ακόμη θα αναλύσουμε τα *a priori* και *a posteriori* σφάλματα για γραμμικά προβλήματα, καθώς υπάρχει έλλειψη των εννοιών αυτών σε πιο περίπλοκα και μη–γραμμικά συστήματα. Θα αναφερθούμε επιπλέον στις συναρτήσεις βάσεις που μας βοηθούν να διακριτοποιήσουμε το πρόβλημα μας και στα είδη στοιχείων που προκύπτουν.

Θα ξεκινήσουμε την αριθμητική επίλυση με τη βαθμωτή εξίσωση Advection–Diffusion, που παρουσιάζει δυσκολίες στην επίλυσή της. Για να προσπεράσουμε το εμπόδιο αυτό θα παρουσιάσουμε κάποιες παραλλαγές της μεθόδου των Πεπερασμένων Στοιχείων όπως τη Stabilized Upwind Petrov–Galerkin (SUPG), την Galerkin Least Squares (GLS) και την Unusual Stabilized FEM(USFEM).

Στο τέταρτο κεφάλαιο θα ασχοληθούμε με τις εξίσωσεις Navier–Stokes. Θα παρουσιάσουμε τον φορμαλισμό της εξίσωσης με την κλασική μέθοδο των Πεπερα-

σμένων Στοιχείων και τις επεκτάσεις SUPG και Variational Multiscale Scheme (VMS). Επιπλέον θα αναφερθούμε στην Discontinuous Galerkin (DG).

Θα συνεχίσουμε παρουσιάζοντας ένα φάσμα προβλημάτων δοκιμής για τις εξισώσεις αυτές, όπως εκείνα της κίνησης σε δοχείο με κινούμενο άνω άκρο (driven cavity) και του backward step. Στόχος μας είναι να δείξουμε ότι η μέθοδος αυτή μας παρέχει αξιόπιστα αποτελέσματα σε όλες τις περιπτώσεις.

Τέλος θα επικεντρωθούμε στις εφαρμογές της μεθόδου σε προβλήματα Εμβιομηχανικής. Θα ασχοληθούμε με μία τρισδιάστατη δομή καρωτίδας που έχει προκύψει από αναδόμηση της πραγματικής δομής. Θα παρουσιάσουμε τα αποτελέσματα που προέκυψαν από την αριθμητική λύση του προβλήματος χρησιμοποιώντας την SUPG.

Τα αποτελέσματα και οι εικόνες προέκυψαν με την χρήση των προγραμμάτων MATLAB, FEniCS, SimVascular, WOLFRAM MATHEMATICA, GeoGebra και LaTeX.

Abstract

The finite element method is a numerical method for calculating approximate solutions of partial differential equations (PDE's). This method is a powerful tool in the study of various problems and finds a large number of applications. We will concentrate here on applying the method to Fluid Mechanics problems. Fluid Mechanics is a particular branch of classical mechanics which has as main object of research and study the static and dynamic behavior of fluids. Fluid is characterized as any substance presenting a flow, i.e. refers to liquids and gases whose cohesion forces are weak, so that they each take the shape of the space they occupy or the medium through which they move.

In this thesis, we will attempt to solve the differential equations describing fluid movement. However, since the solution of these equations is not always possible, as in the case of the Navier–Stokes equations, it is necessary to extend to new ways of solving them, such as the Finite Element method. First we will present the method along with the basic theorems of existence and uniqueness of the solutions that arise.

We will also analyze the *a priori* and *a posteriori* errors for linear problems only, as there is a lack of these concepts in more complex systems. We will also refer to baseline functions that help us to distinguish the problem and the types of data that arise.

We will begin the numerical solution with the Advection–Diffusion scalar equation, which presents difficulties in solving it. To overcome this obstacle, we will also present finite element method variants such as the Stabilized Upwind Petrov–Galerkin (SUPG), Galerkin Least Squares (GLS) and Unusual Stabilized FEM (USFEM).

In the fourth chapter we will deal with the Navier–Stokes equations. We will present the formulation of the equation in the classical method of Finite Element and the advancements of SUPG and Variational Multiscale Scheme. In addition, we will discuss about the Discontinuous Galerkin (DG).

We will continue by presenting a range of test problems for these equations, such as the driven cavity and the backward step. Our goal is to show that these methods provide reliable numerical results in all cases and extended ranges of dimensionless numbers, such as the Reynolds number.

Finally, we will concentrate on the application of the method in a problem of the biomedical field. We will deal with a three–dimensional patient–based carotid structure and present the results obtained from the numerical solution of the problem using the SUPG method.

The obtained results and images resulted from the use of the programs MATLAB, FEniCS, SimVascular, WOLFRAM MATHEMATICA, GeoGebra and LaTeX.

Contents

Περίληψη **i**

Abstract **iii**

1 Introduction **3**

1.1 The Weighted Residual Method 3

1.2 The Finite Element Method 4

1.3 FEM in Fluid Mechanics 5

2 Theory and Principals of the Finite Elements **9**

2.1 Basic Theory 10

2.1.1 Error Estimates 15

2.1.2 Shape Functions 16

2.2 The Stokes Problem 22

2.2.1 A priori error estimates 24

2.2.2 A posteriori error estimates 26

2.2.3 Crouzeix–Raviart finite element discretization and finite volume scheme 28

3 Advection-Diffusion Equation **33**

3.1 The advection–diffusion equation 33

3.1.1 The Galerkin Formulation 34

3.1.2 The Stabilized Finite Element Methods, SUPG & GLS . 34

3.2 Test problem for the advection–diffusion equation 37

4 Navier-Stokes Equations **41**

4.1 Streamline–Upwind/Petrov–Galerkin (SUPG) 42

4.2 Stabilized FEM and the Variational multiscale method (VMS) 43

4.3 Discontinuous and adaptive Galerkin method 44

4.4 Test problems and applications 46

4.4.1 The backward step test problem 46

4.5 Application in Biomedical Engineering 49

4.5.1 Reconstruction of the carotid artery 49

4.5.2 Mathematical Formulation and boundary conditions . . 49

4.5.3 Sensitivity Analysis 50

4.5.4 FEM unsteady simulations 52

4.6 Results and discussion 53

5 Conclusions **57**

Appendix A **59**

Appendix B **61**

Bibliography **63**

CHAPTER 1

INTRODUCTION

1.1 The Weighted Residual Method

The Weighted Residual Method or WRM is a generic class of numerical methods. The WRM is illustrated on a simple one–dimensional problem. Let's assume that a mathematical problem is governed by the following differential equation,

$$L(u) = 0,$$

and it is to be solved over a given domain, D, subject to the initial and boundary conditions, respectively,

$$I(u) = 0, \;\; B(u) = 0,$$

where, L, I and B denote operators of the function u. An appropriate solution $\hat{u}$ can be introduced in the above relations providing the following residuals or errors,

$$L(\hat{u}) = R \neq 0, \;\; I(\hat{u}) = R_I \neq 0, \;\; B(\hat{u}) = R_B \neq 0.$$

Then the approximate solution can be structured so that,

1. $R = 0$, then it is called a boundary method.
2. $R_B = 0$, then it is called an interior method.
3. Else it is a mixed method.

Focusing on the interior in the following analysis of WRM, the approximate solution is taken as,

$$\hat{u}(x) = u_0(x,t) + \sum_{j=1}^{J} a_j(t)\phi_j(x),$$

where $a_j(t)$ are unknown coefficients, $\phi_j(x)$ are called trial functions, and $u_0(x,t)$ must satisfy the given initial and boundary conditions.

In WRM, the coefficient $a_j(t)$ are determined by setting the weighted average of the residual of the equation over the computational domain equal to zero, such as in the following equation,

$$\int_{\Omega} w_k(x)\ R\, dv = 0, \quad for\ \ k = 1, ..., J.$$

Some variants of the Weighted Residual Methods are the following:

1. the Subdomain method, one example of this is the Finite Volume method.
2. the Collocation method, the residual is forced to be zero at specific locations.
3. the Least–Square method.
4. the method of Moments.
5. the Galerkin and Ritz methods.
6. the Petrov–Galerkin method.
7. the Spectral methods.

In this dissertation, we mainly focus our attention on the Galerkin, Ritz and Petrov–Galerkin methods. The Finite Element Method as an extension of the WRM, has been based and developed from the aforementioned methods [25, 26]. Studying or analyzing a phenomenon with FEM is often referred to as finite element analysis (FEA).

1.2 The Finite Element Method

Finite element method (FEM) has gained substantial momentum in the last decades. FEM was initially introduced as an answer to solid mechanics problems that were difficult to solve until then. Most of them would be encountered in aeronautics or civil engineering due to the need of solving problems related to the construction of complicated structures. The method was extended to fluid mechanics applications where the convective terms play important role

leading to a non–linear formulation of the problem. The progress in fluid mechanics was slower due to the non–linearities and instabilities of the solution of these problems.

The basic principles of the FEM were developed by the German mathematician Ritz in 1909. In 1915 Galerkin worked on the theoretical aspects of the method. The absence of computers delayed further advancement of the method. Later on, when computers were introduced, the method was further developed. Hrenikoff, 1941, introduced the framework method, in which a plain elastic medium could be replaced by an equivalent system of sticks and rods. In 1943 Courant solved the torsion problem by using triangular elements based on the principal of minimum potential energy introducing the Rayleigh–Ritz method. Courant's theory could not be implemented due to the unavailability of computers at the time

Argyris, 1955, in the book "Energy Theorems and Structural Analysis" introduced the principals of the finite element method [2, 59]. In 1956 Clough, Turner, Martin and Top calculated the stiffness matrix of rod and other elements. Argyris and Kelsey, 1960, published their work which was based on the finite element principles. In the same year, the term Finite Element Method was introduced by Clough in his paper and the term has been used extensively in the literature until today. Zienkiewicz and Chung wrote the first book on finite elements method, in 1967. Zlámal, worked also on the finite element method with very interesting results [67]. Other notable researchers in the FEM field are Samuel Levy, Borje Langefors, Paul Denke, Baudoin Fraejis De Veubeke, L. Brandeis Wehle Jr., Theodore Pian, Warner Lansing, Bertran Klein, John Archer, Robert Melosh, John Przemieniecki, Ian Taig, Richard Gallagher, Bruce Irons, and others.

1.3 FEM in Fluid Mechanics

As mentioned before the progress of FEM in fluid mechanics applications had several drawbacks due to the non–linear convective terms and instabilities of the solution based on the element selection. For these reasons many researchers studied the advection–diffusion equation. The Galerkin method was introduced as a natural extension of the weak formulation of the PDEs under consideration. One of the reasons why finite elements have been less popular in the past than other numerical techniques such as finite differences, is the lack of upwind techniques. However, accurate upwind methods have been

constructed. The most popular of these upwind approaches is the Streamline Upwind Petrov–Galerkin method (SUPG) [63]. It can be shown that upwinding may increase the quality of the solution considerably. Another important aspect of upwinding is that it makes the systems of equations appropriate for the utilization of iterative methods. As a consequence both the number of iterations and the computation time substantially decrease.

The advection–diffusion equation represents diffusion of a scalar variable while convected by a velocity field. In this respect, the equation by itself applies in several physical phenomena and is a precursor to studying the non–linear Navier–Stokes equations that represent in a simplifying manner the transport of velocity itself. In any case, the development of accurate and stable numerical formulations for the advection–diffusion equation is quite challenging. For example, the classical Galerkin method is known to perform poorly for advection–dominated transport problems. Spurious oscillations emerge in the solution due to the truncation error inherently introduced in the discretized Galerkin approximation. The literature suggest numerous strategies to overcome this problem. The addition of artificial diffusion is a standard strategy, another is the employment of a non-centered discretization of the advection operator, the so-called upwind schemes [32]. Other strategies involve multiscale models using bubble functions or wavelets [52], while in many cases, these methods are equivalent [14]. In the relevant section of this chapter, more information is provided regarding some of the strategies in the context of finite element methods that have been developed to address the problems that standard discretizations face.

Studying the advection–diffusion equation helps in understanding more complicated problems such as the Navier–Stokes equations. For the discretization of the incompressible Navier–Stokes equations, since the pressure is an unknown in the momentum but not in the continuity equation, the discretization must satisfy some special requirements. In fact one is no longer free to choose any combination of pressure and velocity approximation but the finite elements must be constructed such that the Ladyzhenskaya–Brezzi–Babuska (LBB) condition is satisfied. This condition provides a relation between pressure and velocity approximation. In finite differences and finite volumes the equivalent of the LBB condition is satisfied if staggered grids are applied.

The divergence free approach has been introduced where in this method, the elements are constructed in such a way that the approximate divergence freedom is satisfied explicitly. This method seems very attractive, however, the extension to three-dimensional problems is a difficult task. Stabilized

and multiscale formulations are among the most fundamental methods for fluid mechanics problems. The SUPG is one of the first finite element approaches for studying fluid mechanics applications. However, due to the advancement in research nowadays, new finite element approaches have emerged such as the Variational Multiscale Method (VMS), the Characteristic Base Split (CBS) method, the Gradient Smoothed Method (GSM) and the discontinuous Galerkin (DG) and adaptive FEM.

In this dissertation we initially present the basic analysis of the Finite Element Method focused on the Stokes problem providing error estimates. Further three Finite Element approaches are presented and analysed, the Classical Galerkin, the SUPG and the Galerkin Least Squares (GLS). The last two are some of the oldest and more developed approaches. A comparative analysis follows among these three approaches on a simple domain solving a Dirichlet problem. A similar analysis follows for the non–linear Navier–Stokes equations in which we focus on the Chorin splitting method and a stabilized method, the SUPG. These advancements will help study two–dimensional test problems as well as a three–dimensional patient–based structure. We conclude this dissertation with the final results and arguments for the Finite Element Method.

CHAPTER 2

Theory and Principals of the Finite Elements

This chapter is dedicated to the basic principals of the finite element method. In the beginning, we formulate basic definitions and theorems about the existence and uniqueness of the solution in these problems. More details can be found in the textbooks by Brenner & Scott and Brezzi [13, 15].

The governing equation of most of the physical problems are usually represented by using partial differential equations (PDE). This along with the boundary conditions together is called the strong form of the differential equation. The strong form in its original avatar imposes differentiability and continuity requirements on its solutions. Incorporating boundary conditions is always a challenging task with solving strong forms directly. The name "strong form" is probably because of the stronger requirements on the continuity of field variables.

To counter these difficulties, weak formulations are preferred. The weak form is a mathematical manipulation to relax the "strong" requirements for the solution of a PDE. The weak form reduces the continuity requirements on the basis functions used for approximation which gives way to using lesser degree polynomials. This is done by converting the differential equation into an integral form which is usually easier to solve comparatively.

2.1 Basic Theory

Consider the following boundary value problem

$$\begin{cases} -\dfrac{d^2u}{dx^2} = f, x \in (0,1) \\ u(0) = 0 \\ u'(1) = 0 \end{cases} \tag{2.1}$$

We multiply both parts of the equations with function (test function) v with $v(0) = 0$ and by integrating the result we obtain

$$\int_0^1 f(x)v(x)dx = \int_0^1 -u''(x)v(x)dx$$

$$\int_0^1 u'(x)v'(x)dx + u'(x)v(x)\Big|_0^1 = \int_0^1 f(x)v(x)dx := (f,v)$$

The term $u'(x)v(x)\Big|_0^1$ is equal to zero because $u'(1) = 0, v(0) = 0$.

Thus,

$$(f,v) = \int_0^1 u'(x)v'(x)dx =: a(u,v)$$

where

$$a(u,v) = \int_0^1 u'(x)v'(x)dx \tag{2.2}$$

is a **bilinear form**.

Let us define the function space

$$V = \left\{ v \in L^2(0,1) : a(v,v) < \infty \;\; and \;\; v(0) = 0 \right\}$$

as the **test space**.

$L^2(0,1)$ is the space of **square integrable** functions in $[0,1]$. It can be proved that these functions can create a Banach space (complete function space with metric). In the case that is enforced with an inner product, then the space is called Hilbert(and is the same as a H^1 Sobolev space). The inner product in L^2 is defined as:

$$< f, g >_{L_2} = \int_0^1 f \; g \; dx.$$

We need to find a $u \in V$ such that

$$a(u, v) = (f, v), \quad \forall v \in V. \tag{2.3}$$

This form (2.3) is called the **variational** or **weak form** of the equation.

Definition 2.1.1. Let $a(\cdot, \cdot)$ be a bilinear form on a normed linear space, H. The bilinear form is said to be **bounded** (or **continuous**) if there exists a $C < \infty$ such that,

$$\mid a(u, v) \mid \leq C \, \|u\|_H \, \|v\|_H \quad \forall \, u, v \in H,$$

and **coercive** on the subspace $V = \left\{ v \in H^1(0, 1) : v(0) = 0 \right\}$, $V \subset H$ if there exists a $\delta > 0$ such that,

$$a(v, v) \geq \delta \, \|v\|_H^2 , \quad \forall \, v \in V,$$

where $\|\cdot\|_H$ is the norm in the space H.

Focusing our attention on the non–symmetric variational problem, that is more general, the following conditions are valid,

$$\begin{cases} (H, (\cdot, \cdot)) \text{ is a Hilbert space.} \\ V \text{ is a (closed) subspace of } H. \\ a(\cdot, \cdot) \text{ is a bilinear form on } V. \\ a(\cdot, \cdot) \text{ is continuous (bounded) on } V. \\ a(\cdot, \cdot) \text{ is coercive on } V. \end{cases}$$

Then the non–symmetric variational problem is the following, given $F \in V'$, find $u \in V$, such that,

$$a(u, v) = F(v), \forall \, v \in V, \tag{2.4}$$

where V' is the dual space of V.

The discrete form or the Galerkin approximation, of this problem is the following, given a finite dimensional subspace $V_h \subset V$ and $F \in V'$, find $u_h \in V_h$ such that,

$$a(u_h, v) = F(v), \quad \forall \, v \in V_h. \tag{2.5}$$

Existence and uniqueness, of the solution for both the variational and the approximation problems under the conditions mentioned previously, can be proved with the following theorem [13, 15].

Theorem 2.1.1. ***(Lax-Milgram)*** *Given a Hilbert space $(V, (\cdot,\cdot))$, a continuous, coercive bilinear form $a(\cdot,\cdot)$ and a continuous linear functional $F \in V'$, there exists a unique solution $u \in V$, such that,*

$$a(u, v) = F(v), \quad \forall\, v \in V. \tag{2.6}$$

Before proving the theorem it is necessary to mention the following Lemma and Theorem.

Lemma 2.1.2. ***(Contraction Mapping Principle)*** *Given a Banach space V and a mapping $T : V \to V$ satisfying*

$$\|Tu_1 - Tu_2\| \leq M \|u_1 - u_2\| \tag{2.7}$$

for all $u_1, u_2 \in V$ and fixed $0 \leq M < 1$, there exists a unique $u \in V$ such that

$$u = Tu. \tag{2.8}$$

Thus the contraction mapping T has a unique fixed point u.

Theorem 2.1.3. ***(Riesz Representation Theorem)*** *Any continuous linear functional L on a Hilbert space H can be represented uniquely as*

$$L(v) = (u, v) \tag{2.9}$$

for some $u \in H$. Furthermore, we have

$$\|L\|_{H'} = \|u\|_H \tag{2.10}$$

Remark. According to the Riesz Representation Theorem, there is a natural isometry between H and H' ($u \in H \longleftrightarrow L_u \in H'$). For this reason, H and H' are often identified. For example, we can write $W_2^m(\Omega) \cong W_2^{-m}(\Omega)$(although they are completely different Hilbert spaces). We will use τ to represent the isometry from H' onto H.

Proof. For any $u \in V$, define a functional Au by $Au(v) = a(u, v)$, $\forall v \in V$. Au is linear since

$$\begin{aligned} Au(\gamma v_1 + \delta v_2) &= a(u, \gamma v_1 + \delta v_2) \\ &= \gamma a(u, v_1) + \delta a(u, v_2) \\ &= \gamma Au(v_1) + \delta Au(v_2), \quad \forall v_1, v_2 \in V, \gamma, \delta \in \mathbb{R}. \end{aligned}$$

Au is also continuous since, for all $v \in V$,

$$|Au(v)| = |a(u,v)| \leq C \|u\| \|v\|,$$

where C is the constant from the definition of continuity for $a(\cdot,\cdot)$. Therefore,

$$\|Au\|_{V'} = \sup_{v \neq 0} \frac{|Au(v)|}{\|v\|} \leq C \|u\| < \infty$$

Thus, $Au \in V'$. Similarly, one can show that the mapping $u \to Au$ is a linear map from V to V' which is continuous with $\|A\|_{L(V,V')} \leq C$. Now, by the Riesz Representation Theorem, for any $\phi \in V'$ there exists a unique $\tau\phi \in V$ such that $\phi(v) = (\tau\phi, v)$ for any $v \in V$. We must find a unique u such that

$$Au(v) = F(v) \quad \forall v \in V$$

In other words, we want to find a unique u such that

$$Au = F \quad (\in V')$$

or

$$\tau Au = \tau F \quad (\in V)$$

since $\tau : V' \longrightarrow V$ is a one-to-one mapping. Based on the Contraction Mapping Principle we solve this last equation. We want to find $\rho \neq 0$ such that the mapping $T : V \longrightarrow V$ is a contraction mapping where T is defined by

$$Tv := v - \rho(\tau Av - \tau F) \, \forall v \in V. \tag{2.11}$$

If T is a contraction mapping then there exists a unique $u \in V$ such that

$$Tu = u - \rho(\tau Au - \tau F) = u, \tag{2.12}$$

that is $\rho(\tau Au - \tau F) = 0$, or $\tau Au = \tau F$. It remains to show that such a $\rho \neq 0$ exists. For any $v_1, v_2 \in V$, let $v = v_1 - v_2$. Then

$$\begin{aligned}
\|Tv_1 - Tv_2\|^2 &= \|v_1 - v_2 - \rho(\tau A v_1 - \tau A v_2)\|^2 \\
&= \|v - \rho(\tau A v)\|^2 \\
&= \|v\|^2 - 2\rho(\tau A v, v) + \rho^2 \|\tau A v\|^2 \\
&= \|v\|^2 - 2\rho A v(v) + \rho^2 A v(\tau A v) \\
&= \|v\|^2 - 2\rho a(v, v) + \rho^2 a(v, \tau A v) \\
&\leq \|v\|^2 - 2\rho\gamma \|v\|^2 + \rho^2 C \|v\| \|\tau A v\| \\
&\leq (1 - 2\rho\gamma + \rho^2 C^2) \|v\|^2 \\
&= (1 - 2\rho\gamma + \rho^2 C^2) \|v_1 - v_2\|^2 \\
&= M^2 \|v_1 - v_2\|^2
\end{aligned}$$

Here, γ is the constant in the definition of coercivity of $a(\cdot, \cdot)$. Note that $\|\tau\| \, Av = \|A\| \, v \leq C \|v\|$ was used in the last inequality. We thus need

$$1 - 2\rho\gamma + \rho^2 C^2 < 1$$

for some ρ, i.e, $\rho(\rho C^2 - 2\gamma) < 0$. If we choose $\rho \in \left(0, 2\gamma/C^2\right)$ then $M < 1$ and the proof is complete. □

Remark. The variational (2.4) as well as the approximation (2.5) problems have a unique solution, under the conditions of the non–symmetrical problem.

If $a(u, v)$ is bounded, symmetric and coercive on V then we can have the symmetric variational problem

$$\begin{cases}
(H, (\cdot, \cdot)) \text{ is a Hilbert space.} \\
V \text{ is a (closed) subspace of } H. \\
a(\cdot, \cdot) \text{ is a bounded, symmetric and coercive bilinear form on } V.
\end{cases}$$

In higher dimensional problems the variational form becomes

$$a(u, v) = \int_\Omega A(x) \nabla u(x) \cdot \nabla v(x) + (\mathbf{B}(x) \cdot \nabla u(x)) \, v(x) + C(x) u(x) v(x) \, dx \tag{2.13}$$

where $A, \mathbf{B}, C$ are bounded and measurable functions on $\Omega \subset \mathbb{R}^n$ and $\mathbf{B}$ is a vector. According to Hölder's inequality $a(\cdot, \cdot)$ is continuous on $H^1(\Omega)$ with the constant C depending only on the $L^\infty(\Omega)$ norms of the coefficients.

The coercivity can be on the symmetric form, $\mathbf{B} \equiv 0$ and the existence of a constant $\gamma > 0$ such that,

$$A(x) \geq \gamma \quad and \quad C(x) \geq \gamma \quad for \quad a.a \quad x \in \Omega. \tag{2.14}$$

In the case where $\mathbf{B}$ is nonzero Hölder's inequality becomes

$$\begin{aligned} |\int_{\Omega} (\mathbf{B}(x) \cdot \nabla u(x))\, u(x) dx| &\leq \|B\|_{L^{\infty}(\Omega)} \|u\|_{H^1(\Omega)} \|u\|_{L^2(\Omega)} \\ &\leq \|B\|_{L^{\infty}} \|u\|^2_{H^1(\Omega)}/2 \end{aligned}$$

If (2.14) holds and

$$\||B|\|_{L^{\infty}} \leq 2\gamma \tag{2.15}$$

then $a(\cdot, \cdot)$ is coercive on $H^1(\Omega)$.

Thus uniqueness of the solution can be proved by the following theorem,

Theorem 2.1.4. *If* (2.14) *and* (2.15) *hold, then there is a unique solution, u, to the variational problem with $a(\cdot, \cdot)$ as above and $V = H^1(\Omega)$.*

2.1.1 Error Estimates

We define the **energy norm**, $\|\cdot\|_E$ as,

$$\|v\|_E = \sqrt{a(v, v)}, \quad \forall\, v \in V. \tag{2.16}$$

Based on the above definition for the energy norm and with the use of the Schwartz' inequality the error estimate for the previous problem (2.6) is proven to be,

$$\|u - u_h\|_E = \inf\{\|u - v\|_E : v \in S\}, \tag{2.17}$$

where u is the solution and u_h the approximate one and $v \in S$, S a finite dimensional subspace of V. This is the basic error estimate and is optimal in the energy norm. Moreover, in some cases it can be proved that we can replace "infimum" with "minimum", more details can be found elsewhere [13],

$$\|u - u_h\|_E = \min\{\|u - v\|_E : v \in S\}. \tag{2.18}$$

2.1.2 Shape Functions

Since we work in Sobolev spaces, there are functions that have discontinuities. Thus we need to concentrate on Piecewise Polynomial Spaces. Let a partition of $[0,1]$ with $0 = x_0 < x_1 < ... < x_n = 1$ and let V_h be a linear space of functions v such that:

- $v \in C^0([0,1])$
- $v\,|_{[x_{i-1},x_i]}$ is a linear polynomial and
- $v(0) = 0$

We can define ϕ_i for all $i = 1, ..., n$ and $\phi_i(x_j) = \delta_{ij}$, Kronecker's delta. The purpose of this space is to construct an orthonormal basis $\{\phi_i : 1 \leq i \leq n\}$ for the V_h space. This is called **nodal basis** and the points x_i are called **nodes**.

The purpose of creating a basis is to help in describing the functions that are used, in a discrete space.

There is also a need to find a more efficient way to make our calculations simultaneously and as uniformly as possible due to the fact that sometimes the coordinates of each element can make the problem more complex. Thus, to overpass those difficulties, we introduce the following index,

$$i(e, j) = e + j - 1,$$

which helps to transfer the location of each element into the interval of $[0,1]$. In the following example we can observe the transition from the interval $[2,3]$ to $[0,1]$

$$i(e, 0) = 2$$

$$i(e, 1) = 3$$

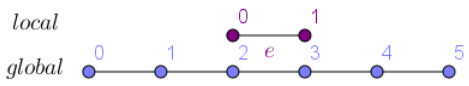

Figure 2.1: Transition from the global to the local system

As we work in discrete intervals we have to transform every function involved to its discrete form. This could happen using the nodal basis. Thus we have

Definition 2.1.2. Given $v \in C^0([0,1])$, then $v_I \in V_h$ is the interpolant of v and is determined by

$$v_I := \sum_{i=1}^{n} v(x_i)\phi_i.$$

Remark. If $v \in V_h \Rightarrow v = v_I$. This happens because $v - v_I$ is linear on each interval $[x_{i-1}, x_i]$ and equal to zero at the endpoints.

We can also define the interpolant of f and is f_I

$$f_I := \sum_{e} \sum_{j=0}^{1} f\left(x_{i(e,j)}\right) \phi_j^e \tag{2.19}$$

where $\{\phi_j^e : j = 0, 1\}$ is the basis of the interval $I_e = [x_{e-1}, x_e]$:

$$\phi_j^e(x) = \phi_j((x - x_{e-1})/(x_e - x_{e-1}))$$

and

$$\phi_0(x) = \begin{cases} 1 - x, & x \in [0,1] \\ 0, & \text{else} \end{cases} \qquad \phi_1(x) = \begin{cases} x, & x \in [0,1] \\ 0, & \text{else} \end{cases}$$

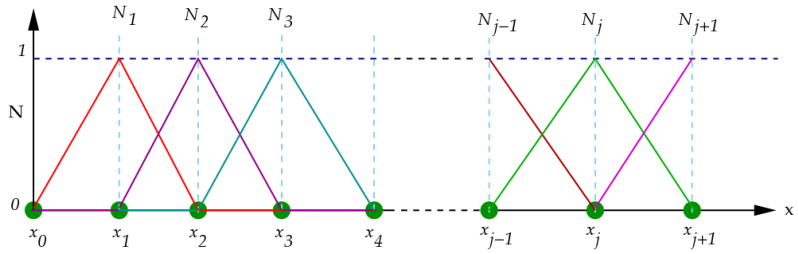

Figure 2.2: Basis

At last we have to convert the bilinear form $a(u, v)$.

$$a(u, v) = \sum_{e} a_e(u, v)$$

where $a_e(u, v)$ is the local bilinear form in each element defined by the following

$$\begin{aligned}
\mathrm{a}_e(u,v) &:= \textstyle\int_{I_e} u'v'\,dx \\
&= (x_e - x_{e-1})^{-1} \textstyle\int_0^1 \left(\sum_j u_{i(e,j)}\phi_j\right)' \left(\sum_j v_{i(e,j)}\phi_j\right)'\,dx \\
&= (x_e - x_{e-1})^{-1} \begin{pmatrix} u_{i(e,0)} \\ u_{i(e,1)} \end{pmatrix}^t K \begin{pmatrix} v_{i(e,0)} \\ v_{i(e,1)} \end{pmatrix},
\end{aligned}$$

where K is the local stiffness matrix

$$K_{i,j} := \int_0^1 \phi'_{i-1}\phi'_{j-1}\,dx, \quad i,j = 1,2.$$

The solution of the problem results by solving the above system.

Definition 2.1.3. Let

i $K \subseteq \mathbb{R}^n$ be a bounded closed set with nonempty interior and piecewise smooth boundary (the **element domain**),

ii $\mathcal{P}$ be a finite-dimensional space of functions on K (the space of **shape functions**) and

iii $\mathcal{N} = \{N_1, N_2, ..., N_k\}$ be a basis for $\mathcal{P}'$ (the set of **nodal variables**).

Then $(K, \mathcal{P}, \mathcal{N})$ is called a **finite element**

Definition 2.1.4. Let $(K, \mathcal{P}, \mathcal{N})$ be a finite element. The basis $\{\phi_1, \phi_2, ..., \phi_k\}$ of $\mathcal{P}$ dual to $\mathcal{N}$ is called the **nodal basis** of $\mathcal{P}$.

In FEniCS the element family and shape function space is determined by the following

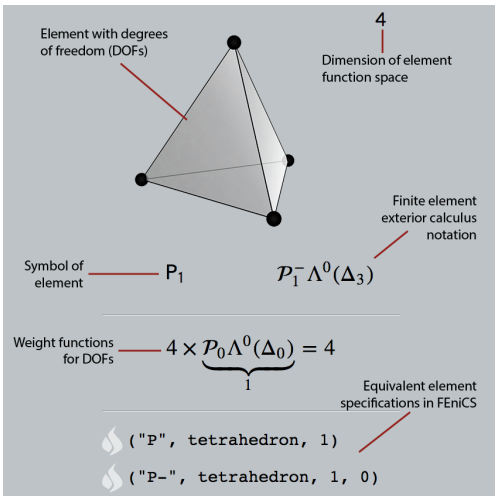

Figure 2.3: Legend of the elements

The family of elements that is used in our algorithms is the $\mathcal{P}_r\Lambda^k$

This space consists of all the differential $k-$forms with polynomial coefficients of degree at most r and the dimension is

$$\dim \mathcal{P}_r\Lambda^k(\Delta_n) = \binom{r+n}{r+k}\binom{r+k}{k}. \tag{2.20}$$

The elements that can be created in this space are the following

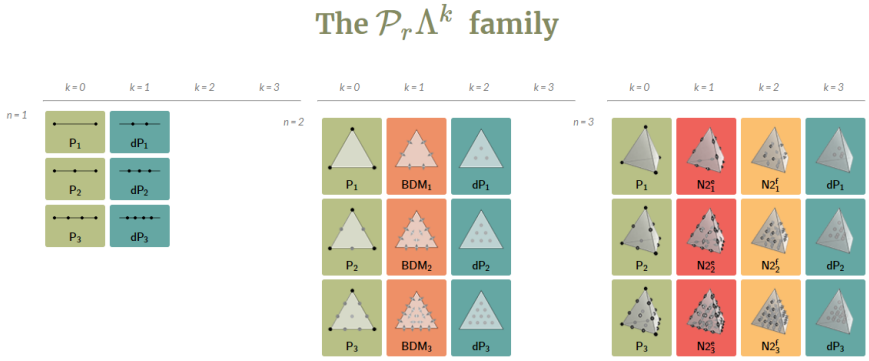

Figure 2.4: The $\mathcal{P}_r\Lambda^k$ family

We observe that in different dimensions we can have either an interval, a triangle or a quadrilateral.

The simplest case is when $k = 0$ and $n = 1$ where we have an interval.

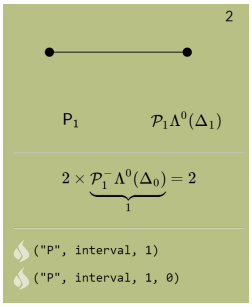

Figure 2.5: Interval element

In higher dimensions

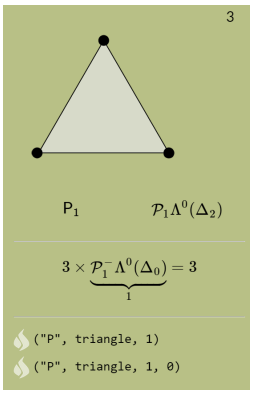

(a) Triangle P_1

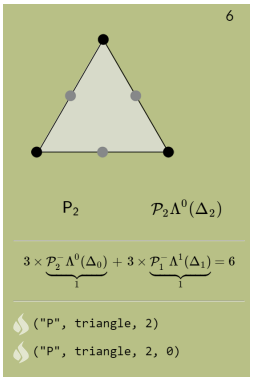

(b) Triangle P_2

Figure 2.6: Triangular Elements

and

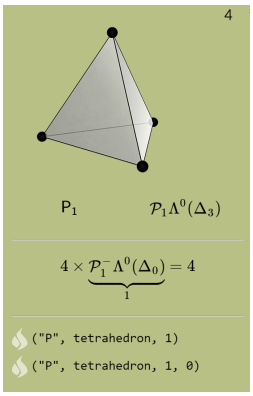

(a) Tetrahedron P_1

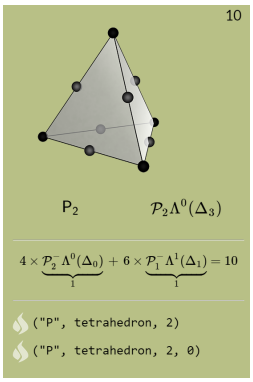

(b) Tetrahedron P_2

Figure 2.7: Tetrahedron Elements

As for the quadrilaterals we have

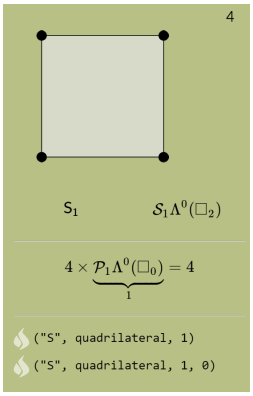

(a) Quadrilateral P_1

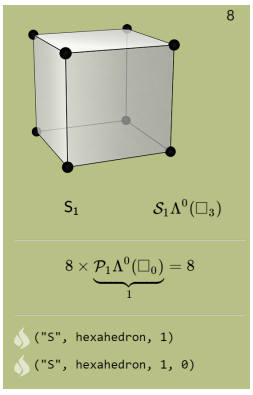

(b) Hexahedron P_2

Figure 2.8: Square Elements

2.2 The Stokes Problem

Initially, we consider the stationary Stokes problem for incompressible flow. Ω is a bounded open set of $\mathbb{R}^n$ (where $n = 2, 3$) with regular boundary and $\mathbf{f}$ is a square integrable function on Ω. We seek a solution $(\mathbf{u}, p) \in H_0^1(\Omega)^2 \times (L^2(\Omega)/\mathbb{R})$ of the problem,

$$\begin{cases} -\Delta \mathbf{u} + \nabla p = \mathbf{f} \quad in \ \ \Omega, \\ \qquad div\, \mathbf{u} = 0 \quad in \ \ \Omega, \\ \qquad\quad \mathbf{u} = 0 \quad on \ \ \partial\Omega. \end{cases}$$

Based on this problem, we will introduce the error estimates (*a priori* and *a posteriori*) and we briefly discuss about the uniqueness of the solution for this problem [8]. Our goal is to extend these arguments for the non–stationary case.

According to the finite element analysis we end up with the following weak form.

$$\begin{cases} a(\mathbf{u}, \mathbf{v}) + b(p, \mathbf{v}) = (\mathbf{f}, \mathbf{v}), & \forall\ \mathbf{v} \in H_0^1(\Omega)^n,\ \mathbf{u} \in H_0^1(\Omega)^n, \\ b(\mathbf{u}, q) = 0 & \forall\ q \in H^1(\Omega),\ p \in H^1(\Omega), \end{cases} \tag{2.21}$$

where, $a(\mathbf{u},\mathbf{v}) = \int_\Omega \nabla\mathbf{u}\,\nabla\mathbf{v}\,d\Omega$ and $b(p,\mathbf{v}) = \int_\Omega p\,\nabla\mathbf{v}\,d\Omega$.

Given two finite dimensional subspaces $V_h \subset H^1(\Omega)^n$ and $Q_h \subset H^1(\Omega)$ the corresponding discrete form is,

$$\begin{cases} a(\mathbf{u}_h,\mathbf{v}_h) + b(p_h,\mathbf{v}_h) = (\mathbf{f},\mathbf{v}_h), & \forall\ \mathbf{v}_h \in V_{0h},\ \mathbf{u}_h \in V_{0h}, \\ b(\mathbf{u}_h,q_h) = 0, & \forall\ q_h \in Q_h,\ p_h \in Q_h, \end{cases} \tag{2.22}$$

where, $V_{0h} = \{\mathbf{v}_h \in V_h : \mathbf{v}_h\,|_{\partial\Omega} = 0\}$.

Two cases are analyzed for both triangular and quadrilateral elements depending on the number of nodes on each element [8]. We focus only on the Taylor–Hood method (six node triangular elements), second order polynomials for the velocity and first order polynomials for the pressure at each element $(P_2 - P_1)$.

After finding a solution, for the problem under consideration, it is important to show that it is stable and how the input data affect it. This can be done using the inf–sup condition, the Ladyzhenskaya–Babuska–Brezzi (LBB) condition. This is a condition for saddle point problems i.e. problems arising in different types of discretization of equations. Convergence is ensured for most discretization schemes for positive definite problems but for saddle point problems there are still discretizations that are unstable, due to spurious oscillations [63]. In these cases a better approach is the adaptation of the computational grid [55]. We further discuss for the BB condition, introducing the following theorem.

Theorem 2.2.1. *If Ω is polygonal and $\Omega_h = \Omega$, $\Omega_h = \bigcup_i T_i$, where T_i are the triangles and h denotes the length of greatest triangle side, if all triangles have at least one vertex which is not on $\partial\Omega$, if V_h, Q_h are chosen as in the Taylor–Hood method, then there exists a constant C, independent of h, such that,*

$$sup_{\mathbf{v}_h \in V_{0h}} \frac{(\mathbf{v}_h, \nabla q_h)}{(\mathbf{v}_h,\mathbf{v}_h)^{\frac{1}{2}}} \geq C\,(\nabla q_h, \nabla q_h)^{\frac{1}{2}}, \quad \forall q_h \in Q_h. \tag{2.23}$$

This theorem follows the idea of the BB condition and the proof depends on the choice of the elements and can be found in [8]. One of the most important questions in solving such a problem is that of existence and uniqueness of the

solution. In this case we focus on the discrete form of the problem under consideration, (2.22) where we can ensure the previous with the following Theorem.

Theorem 2.2.2. *Under the conditions of theorem 2.2.1 the discrete form, equation* (2.22)*, has a unique solution* $(\mathbf{u}_h, p_h)$ *in* $V_{0h} \times (Q_h/\mathbb{R})$ *.*

Additionally, we are interested in error estimates of the Stokes problem as discussed in the next sections.

2.2.1 A priori error estimates

The *a priori* error estimates depend only on the exact solution, but not on the approximated one. On the other hand, the *a posteriori* error estimates require computation of the solution. *A posteriori* error estimates can also provide results on which element size give a larger error contribution leading to conclusions about grid adaptation [55]. A theorem that provides *a priori* error estimates for the discrete form of the stationary Stokes problem using Taylor–Hood elements $(P_2 - P_1)$ is as follows.

Theorem 2.2.3. *Let* Ω *be a polygon and* $\Omega_h = \Omega$ *for all* h*. We assume that each element of* $\mathcal{T}_h$ *(set of triangles) has at least one vertex not on the boundary. Then the following inequalities are valid,*

$$\begin{aligned} \|\nabla(\mathbf{u} - \mathbf{u}_h)\|_0 &\leqslant h^2 K \left(\|\mathbf{u}\|_{H^3(\Omega)^N} + \|p\|_{H^2(\Omega)/R} \right), \\ \|\nabla(p - p_h)\|_0 &\leqslant hK \left(\|\mathbf{u}\|_{H^3(\Omega)^N} + \|p\|_{H^2(\Omega)/R} \right) \quad . \end{aligned} \tag{2.24}$$

Similar inequalities can be found in the case where we have quadrilaterals [8].

Expanding previous arguments for the non stationary problem we find that there are not as many studies as in the previous case. According to Kemmochi [41] for the non–stationary Stokes problem,

$$\begin{cases} \mathbf{u}_t - \Delta\mathbf{u} + \nabla p = \mathbf{f} \quad in \ \ \Omega \times [0,T], \\ \qquad\qquad div\, \mathbf{u} = 0 \quad in \ \ \Omega \times [0,T], \\ \qquad\qquad\quad \mathbf{u} = 0 \quad on \ \ \partial\Omega \times [0,T], \\ \qquad \mathbf{u}(\cdot,0) = \mathbf{u}_0(\cdot) \quad in \ \ \Omega, \end{cases} \tag{2.25}$$

the error estimates for the velocity $\mathbf{u}$ and pressure p are,

$$\begin{aligned} \|\mathbf{u}-\mathbf{u}_h\|_H &\leqslant Ch^2t^{-1}\|\mathbf{u}_0\|_H\,, \\ \|p-p_h\|_Q &\leqslant Cht^{-1}\|\mathbf{u}_0\|_H \quad . \end{aligned} \tag{2.26}$$

Remark. The difference between the *a priori* error estimates for the stationary and the non-stationary Stokes problem is the introduction of the time variable in the results. Additional results can be obtained for the time derivative for the non-stationary Stokes problem.

In many cases, of the classic finite element approach, the LBB condition is not satisfied, thus its necessary to find a way to solve the problems and also satisfy this condition. An effective way to overcome this problem is to utilize the adaptive FEM. In the following, we analyze the method suggested by Arnold, Brezzi and Fortin for the Stokes problem [4]. The discrete form is,

$$\begin{cases} \displaystyle\sum_{i,j=1}^{2}\int_\Omega \epsilon_{ij}(u)\epsilon_{ij}(v)\,dx - \int_\Omega p\,\nabla\cdot u\,dx = \int_\Omega fv\,dx \quad \forall v\in(H_0^1(\Omega))^2, \\ \displaystyle\int_\Omega q\,\nabla\cdot u\,dx = 0 \quad \forall q\in L^2(\Omega)/R, \end{cases} \tag{2.27}$$

where $\epsilon_{ij}(u) = \dfrac{(\partial_i u_j + \partial_j u_i)}{2}$. This method is based on using the MINI element as a way to satisfy the inf–sup condition introducing an operator $\Pi_h : (H_0^1(\Omega))^2 \to V_h$. Thus the second equation can be written as,

$$\int_\Omega q_h div\,(\Pi_h v - v)\;dx = 0, \quad \forall q_h\in Q_h, \forall v\in\left(H_0^1\right)^2 \tag{2.28}$$

and

$$\|\Pi_h v\|_1 \leq c\,\|v\|_1 \quad \forall v\in\left(H_0^1\right)^2. \tag{2.29}$$

For the MINI element the space is,

$$V_h = \left(\mathring{M}_0^1\right)^2 \oplus \left(B^3\right)^2, \qquad Q_h = M_0^1, \tag{2.30}$$

where,

$$M_0^k(\mathcal{T}_h) = \left\{v \mid v\in C^0(\Omega), v_{|T}\in P_k(T), \;\; \forall\, T\in T_h\right\}, \;\; \mathring{M}_0^k(\mathcal{T}_h) = M_0^k(\mathcal{T}_h)\cap H_0^1(\Omega) \tag{2.31}$$

for $k\geq 1$ and

$$B^k(T_h) = \left\{v \mid v_{|T}\in P_k(T)\cap H_0^1(T), \;\; \forall\, T\in T_h\right\}, \tag{2.32}$$

for $k \geq 3$ and T the triangular elements of $\mathcal{T}_h$. For the problem based on the MINI elements, the following argument is valid,

$$\|u - u_h\|_1 + \|p + p_h\|_{0/R} \leq C \inf \left\{ \|u - v\|_1 + \|p + q\|_{0/R} \right\} \leq Ch \|f\|_0 , \quad (2.33)$$

where C is independent of h. These spaces can be further extended leading to other methods [4]. For example there is a case where it can be seen as an enriched version of Taylor–Hood method where convergence is simpler than the classical Taylor–Hood method. In other methods discontinuous approximation of the pressure is used as mentioned in Crouzeix–Raviart [4, 20].

2.2.2 A posteriori error estimates

In this section we focus our attention on *a posteriori* estimates for the approximation of time dependent Stokes equations. We introduce the notion of the Stokes reconstruction operator and present the error equation that satisfies the exact divergence–free condition described in detail in [39].

The energy technique for *a posteriori* error analysis of finite element discretizations of parabolic problems provides suboptimal rates in the $L^{\infty}(0, T ; L^2(\Omega))$ norm. Makridakis and Nochetto in their study combine energy techniques with appropriate pointwise representation of the error based on an elliptic reconstruction operator which restores optimal order and regularity for piecewise polynomials of degree higher than one [48]. Additionally, Lakkis and Makridakis based on the previous work derive *a posteriori* error estimates for fully discrete approximations of the solutions of linear parabolic equations. The discretization uses finite element spaces that change in time [45]. Akrivis and collaborators presented a refined analysis for quasilinear parabolic problems using FEM [1]. Let's consider the non-stationary Stokes problem for incompressible flow. These equations are discretized in space by the finite elements or the finite volumes method. This problem is still open and directly related to Navier–Stokes equations. This is due to the fact that the *a posteriori* error theory is still in progress as reported by several researchers [9, 23, 39, 45, 48]. We assume the availability of *a posteriori* estimator for the Stokes problem, expressed by the following assumption.

Assumption. Let $(\mathbf{w}, q) \in \mathbf{Z} \times \Pi$ and $(\mathbf{w}_h, q_h) \in \mathbf{Z}_h \times \Pi_h$ be the exact solution and its finite element approximation. For the space X (equal to $\mathbf{H} = (L^2(\Omega))^d$, $\mathbf{V} = (H_0^1(\Omega))^d$, $d = 2, 3$ or $\mathbf{V}'$ the dual space of $\mathbf{V}$), we assume that there exists

a posteriori estimator function, $\mathcal{E}((\mathbf{w}_h, q_h)$ and $\mathcal{E}_{pres}((\mathbf{w}_h, q_h)$, which depend on $(\mathbf{w}_h, q_h)$, $\mathbf{g}$ and the corresponding norm, such that,

$$\|\mathbf{w} - \mathbf{w}_h\|_X \leq \mathcal{E}((\mathbf{w}_h, q_h), \mathbf{g};\ X) \quad and \quad \|q - q_h\|_\Pi \leq \mathcal{E}_{pres}((\mathbf{w}_h, q_h), \mathbf{g};\ \Pi). \tag{2.34}$$

It can be shown that the discrete solution coincides with the continuous solution [39]. In order to define the Stokes reconstruction as introduced by Karakatsani and Makridakis, 2006, we provide the following definitions [39, 33],

Definition 2.2.1. (Stokes operator) Let $\bar{\Delta}:\ \mathbf{H}^2 \cap \mathbf{Z} \subset \mathbf{J} \to \mathbf{J}$ be the Stokes operator, meaning, the L^2-projection of the Laplace operator onto $\mathbf{J}$. Then introducing the discrete version of the Stokes operator $\bar{\Delta}_h : \mathbf{Z}_h \to \mathbf{Z}_h$ by,

$$\left\langle \bar{\Delta}_h \mathbf{v}, \chi \right\rangle = -\alpha(\mathbf{v}, \chi), \quad \forall \chi \in \mathbf{Z}_h. \tag{2.35}$$

Definition 2.2.2. (Stokes reconstruction) For fixed $t \in [0, T]$, let $(\mathbf{U}, P) \in \mathbf{V} \times \Pi$ be the solution of the stationary Stokes problem,

$$\begin{cases} a(\mathbf{U}, \mathbf{v}) + b(\mathbf{v}, P) = \langle \mathbf{g}_h(t), \mathbf{v} \rangle, & \forall\ \mathbf{v} \in \mathbf{V}, \\ b(\mathbf{v}, P) = 0, & \forall\ q \in \Pi, \end{cases} \tag{2.36}$$

where,

$$\mathbf{g}_h = -\Delta_h \mathbf{u}_h - \mathbf{f}_h + \mathbf{f}. \tag{2.37}$$

We call $(\mathbf{U}, P) = (\mathbf{U}(t), P(t))$ the Stokes reconstruction of the discrete velocity and pressure fields, $(\mathbf{u}_h(t), p_h(t))$.

Based on the above definitions Karakatsani and Makridakis, 2006, introduce the following theorem, which provides the error equations based on the *a posteriori* estimator function introduced before [39].

Theorem 2.2.4. *(Error equation) Let* $(\mathbf{U}, P)$ *be the Stokes reconstruction and* $(\mathbf{u}, p)$ *the solution of the Stokes problem which is assumed to be sufficiently regular. If* $\mathbf{e} = \mathbf{U} - \mathbf{u}$ *and* $\varepsilon = P - p$*, then* $(\mathbf{e}, \varepsilon)$ *is the weak solution of the problem,*

$$\begin{cases} \mathbf{e}_t - \Delta \mathbf{e} + \nabla \varepsilon = (\mathbf{U} - \mathbf{u}_h)_t, \\ div\ \mathbf{e} = 0. \end{cases} \tag{2.38}$$

Additionally, $\mathbf{U} - \mathbf{u}_h$ *and* $(\mathbf{U} - \mathbf{u}_h)_t$ *satisfy the following estimates,*

$$\left\| \partial_t^{(j)} (\mathbf{U} - \mathbf{u}_h) \right\|_X \leq \mathcal{E}((\partial_t^{(j)} \mathbf{u}_h, \partial_t^{(j)} p_h),\ \partial_t^{(j)} \mathbf{g}_h;\ X), \quad j = 0,\ 1, \tag{2.39}$$

where X is one of the spaces, $\mathbf{H}$, $\mathbf{V}$ or $\mathbf{V}'$, discussed before and $\mathcal{E}$ is the a posteriori estimator function defined in previous assumption. The proof of this theorem can be found in [39].

Theorem 2.2.5. *($L^\infty(\mathbf{H})$ and $L^2(\mathbf{V})$ norm error estimates) Let's assume that $(\mathbf{u}, p)$ is the solution of the time dependent Stokes problem, Eq. (2.25), and $(\mathbf{u}_h, p_h)$ is the finite element approximation. Let $(\mathbf{U}, P)$ be the solution of the stationary Stokes problem and $\mathcal{E}$ is the a posteriori estimator function defined previously. Then the following a posteriori error bounds hold for, $0 < t \leq T$,*

$$\begin{aligned} \|\mathbf{u}(t) - \mathbf{U}(t)\|^2_{\mathbf{H}} + \int_0^t \|(\mathbf{u} - \mathbf{U})(s)\|^2_{\mathbf{V}}\, ds \\ \leqslant \|\mathbf{u}(0) - \mathbf{U}(0)\|^2_{\mathbf{H}} + \int_0^t \mathcal{E}((\mathbf{u}_{h,t}, p_{h,t}), \mathbf{g}_{h,t}; \mathbf{V}')^2 ds. \end{aligned} \tag{2.40}$$

Additional inequalities and the proof of this theorem can be found in [39].

They additionally provide a theorem for $L^\infty(\mathbf{V})$ norm error estimates and at the same study they discuss about estimates using the parabolic duality argument [23, 64]. In this study two related applications of the reconstruction of the Stokes problem are discussed [39].

2.2.3 Crouzeix–Raviart finite element discretization and finite volume scheme

An *a posteriori* bound for the time dependent Stokes problem under the Crouzeix–Raviart finite element approximation is derived. However, further detailed work is required related to the specific form of possible singularities of the exact solution for this problem [39]. The finite volume (FV) scheme approximations is the Crouzeix–Raviart couple $\mathbf{V}_h \times \Pi_h$. The FV methods rely on local conservation properties of the differential equations under consideration over the "control volume". Integrating over a region $b \subset \Omega$ and utilizing the Green's formula, we obtain the following system for the Stokes problem in the discrete form,

$$\begin{cases} \displaystyle\int_{b_e} \mathbf{u}_{h,t} - \int_{\partial b_e} \nabla \mathbf{u}_h \mathbf{n} + \int_{\partial b_e} p_h \mathbf{n} = \int_{b_e} \mathbf{f}, \quad \forall\ e \in E_h, \\ \displaystyle\int_K div\ \mathbf{u}_h = 0, \quad \forall\ K \in \mathcal{T}_h. \end{cases} \tag{2.41}$$

where z_K is an inner point of $K \in \mathcal{T}_h$, connecting the point with line segmants to the vertices of the triangle K, we partition it into three segmants K_e, where $e \in E_h(K)$, then each side e is associated with a quadrilateral, b_e, which is the union of the subregions K_e. Chatzipandelidis et al. have introduced *a priori* and *a posteriori* error estimates for the FV methods and for the stationary Stokes problem with the admition that FV scheme provides a variational formulation similar to the FE scheme [17]. These studies highlight the importance of *a posteriori* error estimates on a theoretical basis especially for parabolic problems such as the Stokes equation [10, 17].

We highlight the main finding from Karakatsani and Makridakis study [**?**] for the FV scheme that is the following theorem.

The driven cavity test problem for the Stokes equations

The Stokes equation, shown below,

$$-\Delta \mathbf{u} + \nabla p = \mathbf{f},$$

consists of the diffusion terms, $-\Delta \mathbf{u}$, the pressure gradient, ∇p and the external forces, $\mathbf{f}$. The problem we focus in, is the driven cavity. Driven cavity is a benchmark problem for viscous incompressible fluid flow. We are dealing with a square cavity consisting of three rigid walls with no-slip conditions and a lid moving with a tangential unit velocity.

The Stokes problem in the strong form is,

$$\begin{cases} -\Delta \mathbf{u} + \nabla p = \mathbf{f} \quad in \ \ \Omega, \\ \qquad div\, \mathbf{u} = 0 \quad in \ \ \Omega, \\ \qquad\quad \mathbf{u} = 0 \quad on \ \ \partial\Omega \end{cases} \tag{2.42}$$

and the corresponding weak form will be,

$$\begin{cases} a\left(\mathbf{u}, v\right) + b\left(p, v\right) = \left(\mathbf{f}, v\right), & \forall \mathbf{v} \in V = \left\{H_0^1(\Omega)^d\right\} \\ b\left(\mathbf{u}, q\right) = 0 & \forall q \in \Pi = \left\{q \in L^2(\Omega) : \int_\Omega q \, dx = 0\right\} \end{cases} \tag{2.43}$$

where $a\left(\mathbf{u}, v\right) = \int_\Omega \nabla \mathbf{u} \, \nabla v \, d\,\Omega$ and $b\left(p, v\right) = \int_\Omega p \, \nabla v \, d\,\Omega$.

$$a\left(\mathbf{u}, v\right) + b\left(p, v\right) + b\left(\mathbf{u}, q\right) = \left(\mathbf{f}, v\right) \tag{2.44}$$

The new weak form is,

$$Q(\mathbf{u}, p; \mathbf{v}, q) = \left(\mathbf{f}, v\right). \tag{2.45}$$

The results show the formation of a vortex near the center of the square for the velocity field, Figure 2.10. The velocity approaches the maximum value at the top of the cavity, where the fluid flow is being driven by the moving wall. One can see that the fluid is pushed into the wall on the right, where it flows downward before moving back up to the left side of the cavity. This motion creates a large vortex in the center of the cavity [30]. The pressure field solution reveals two discontinuous regions on the left and right corners of the top moving lid. In finest meshes the obtained numerical solution is more accurate. However, increasing the grid resolution would improve the results, but since the boundary conditions are not smooth at the top corners, we will always have discontinuous results for the pressure field, Figure 2.11.

Theorem 2.2.6. *(Residual based $L^2(H^1)$ and $L^\infty(H^1)$ norm error estimates) Let's assume that $(\mathbf{u}, p)$ is the solution of the time dependent Stokes problem and $(\mathbf{u}_h, p_h)$ is the finite volume approximation. The following a posteriori error bounds hold for, $0 < t \leq T$,*

$$\begin{aligned} \|\nabla(\mathbf{u}-\mathbf{u}_h)(t)\|_H \;\leq\; & \left\|\mathbf{u}_0-\mathbf{u}_h^0\right\|_V + C\left(\int_0^t \eta_1(\mathbf{u}_{h,t}(s))^2 ds\right)^{1/2} \\ & + C\,\eta_1\left(\mathbf{u}_h(0)\right) + C\,\eta_1(\mathbf{u}_h(t)), \end{aligned} \tag{2.46}$$

Additional inequalities and the proof of this theorem can be found in [39].

Further, Larson and Malqvist derived a residual based *a posteriori* error estimates for parabolic problems on mixed form using Raviart-Thomas-Nedelec (RTN) finite elements in space and backward Euler in time [46]. In their study an *a posteriori* error estimate for the divergence of the flux in a weak norm is derived. The consept of elliptic reconstruction has been used to derive *a posteriori* error estimates for parabolic problems as briefly described before [39, 48]. In this framework, Larson and Malqvist, use known *a posteriori* error estimates for the corresponding elliptic problem to derive error bounds for the parabolic problem [46]. However, the literature on FEM for parabolic problems on mixed form is less extensive and the development of the theory is still in progress [21, 64].

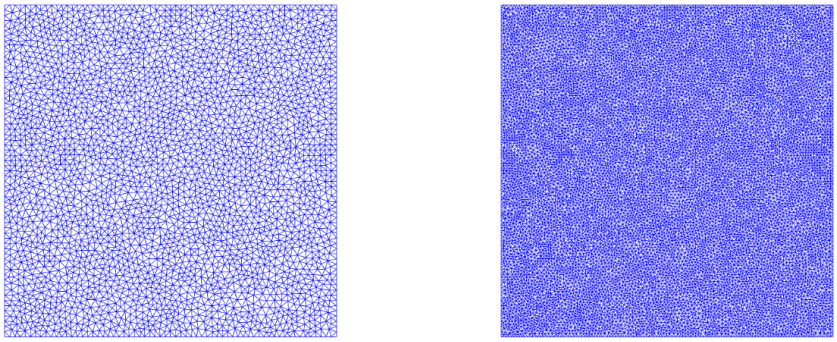

(a) Mesh $(50, 50)$ (b) Mesh $(100, 100)$

Figure 2.9: Meshes

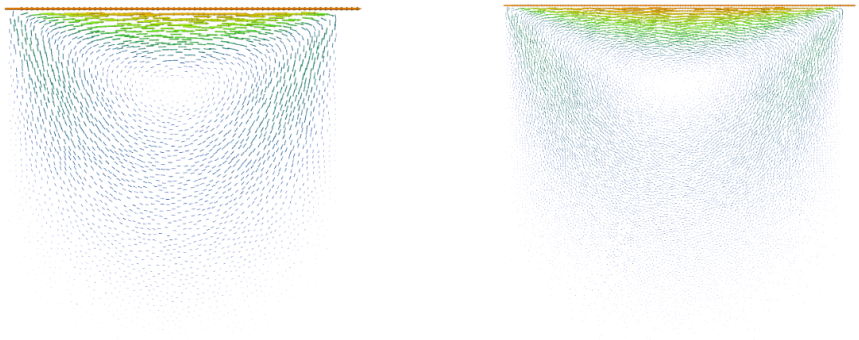

(a) Velocity$(50, 50)$ (b) Velocity $(100, 100)$

Figure 2.10: Velocity Results

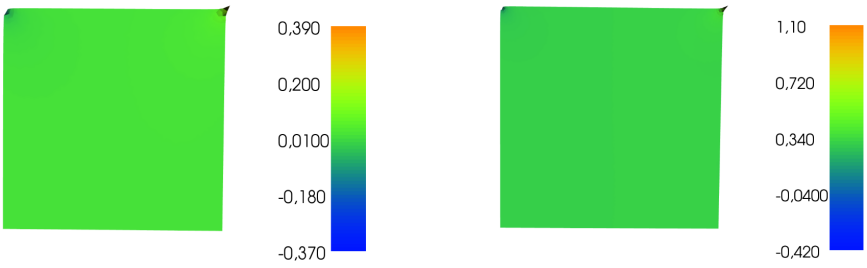

(a) Pressure case a $(50, 50)$ (b) Pressure case b $(100, 100)$

Figure 2.11: Pressure Results

CHAPTER 3

Advection-Diffusion Equation

3.1 The advection–diffusion equation

The steady–state advection and diffusion of a scalar field is described by the partial differential equation (homogeneous Dirichlet boundary condition),

$$\alpha \cdot \nabla u - \nabla \cdot (D \nabla u) = f \qquad \text{in } \Omega \,, \tag{3.1}$$

$$u = 0 \qquad \text{on } \partial\Omega \,, \tag{3.2}$$

where α is the velocity that the quantity, u, is moving with, which is considered to be divergent–free, $\nabla \cdot \alpha = 0$ [14]. For example, take as quantity the concentration of a chemical species that diffuses in a river while moving with its velocity α. The diffusion coefficient of the quantity is denoted with D and f represents sources or sinks.

The advection–diffusion problems are frequently treated as the point of departure for the study of the non-linear Navier–Stokes equations, at the level of developing discretization methods. The Peclet number, defined as the ratio of the advection and diffusion rates, $Pe = |a|h/D$, is a characteristic dimensionless number for such problems. A small Peclet number (Pe $\ll 1$) indicates diffusion-dominated flows while a large one (Pe $\gg 1$) indicates advection–dominated flows. In the diffusion–dominated regime, the standard Galerkin finite element method provides a good approximation of the solution [12].

The standard variational formulation arises by requesting the residual of Eq. (3.1) to be orthogonal to a basis of the function space, H_0^1. The task is to find $u \in H_0^1(\Omega)$ such that,

$$(\alpha \cdot \nabla u, v) - (\nabla \cdot (D\nabla u), v) = (f, v), \tag{3.3}$$

is satisfied for any test function $v \in H_0^1(\Omega)$. The Sobolev space, H_0^1, consists of functions that are one time weakly differentiable and also satisfy the zero Dirichlet boundary condition. In this respect, the second order term of the weak formulation can be integrated by parts, leading to,

$$(\alpha \cdot \nabla u, v) + (D\nabla u, \nabla v) = (f, v). \tag{3.4}$$

3.1.1 The Galerkin Formulation

To approximately solve Eq. (3.4) using the Finite Element method, Ω is discretized in non–overlapping triangle element domains Ω_e with boundaries $\Gamma_e,\ e = 1, 2...K$, such that,

$$\Omega = \bigcup_{k=0}^{K} \overline{\Omega_k}.$$

The standard Galerkin formulation is retrieved by searching a solution in a finite-dimensional linear polynomial function space, $V_h \subset H_0^1(\Omega)$,

$$V_h = \{v_h \in H_0^1(\Omega) \mid v_h(\Omega_k) \in P_1(\Omega_k),\ \Omega_k \in \Omega\}$$

The problem now states, find $u \in V_h(\Omega)$ such that,

$$(\alpha \cdot \nabla u_h, v_h) + (D\nabla u_h, \nabla v_h) = (f, v_h), \qquad \forall\ v_h \in V_h(\Omega). \tag{3.5}$$

3.1.2 The Stabilized Finite Element Methods, SUPG & GLS

It is well known that for advective–dominated flows, where the Peclet number is large, the solution involves non–physical oscillations [14]. To address the deficiency of the standard polynomial finite element method for advection–dominated flow problems, various approaches have been proposed, such as the streamline upwind Petrov–Galerkin (SUPG) method [16], Galerkin least squares (GLS) method [37], and the unusual stabilized FEM (USFEM) [27]. The common characteristic of the aforementioned methods is the introduction

of artificial diffusion in the solution process while preserving the consistency of the discretization. Such methods are commonly referred to as stabilized finite element methods (SFEM).

The SFEM for the stationary advection–diffusion problem can be grouped as follows: find $u_h \in V_h(\Omega)$ such that,

$$B(u_h, v_h) = F(v_h), \qquad \forall\ v_h \in V_h(\Omega), \tag{3.6}$$

where,

$$B(u_h, v_h) = (\alpha \cdot \nabla u_h, v_h) + (D\nabla u_h, \nabla v_h) + Q(u_h, v_h), \tag{3.7}$$

$$F(v_h) = (f, v_h), \tag{3.8}$$

where $Q(u_h, v_h)$ indicates the additional terms added to the standard variational formulation. These are added to preserve consistency and enhance numerical stability. For instance, the stability term corresponding to the SUPG method is,

$$Q_{SUPGF}(u_h, v_h) = \sum_K \tau_k(\alpha \cdot \nabla u_h - \nabla \cdot (k\nabla u_h) - f, \alpha \cdot \nabla u_h)_k, \tag{3.9}$$

where $(\cdot, \cdot)_k$ denotes element wise integration and τ_k is the stability coefficient for the SUPG method, as defined in [28],

$$\begin{cases} \tau_k = \dfrac{h_k}{2|\alpha|_p}\xi(Pe_k), \\ Pe_k = \dfrac{m_k|a|_p h_k}{2k}, \\ \xi(Pe_k) = \begin{cases} Pe_k, & 0 \le Pe_k < 1 \\ 1, & Pe_k \ge 1 \end{cases} \\ |\alpha|_p = \left(\displaystyle\sum_{i=1}^{N} |\alpha_i|_p\right)^{\frac{1}{p}},\ 1 \le p < \infty, \\ m_k = \min\left\{\dfrac{1}{3},\ 2C_k\right\}, \\ C_k \displaystyle\sum_K h_k^2 \left\|\Delta v_h\right\|_{0,K}^2 \leqslant \left\|\nabla v_h\right\|_0^2,\ v_h \in V_h. \end{cases} \tag{3.10}$$

Accordingly, the stability terms added to the standard variational formulation for the GLS and the USFEM methods are,

$$\begin{cases} Q_{GLS}(u_h, v_h) = \sum_K \tau_k(\alpha \cdot \nabla u_h - \nabla \cdot (D\nabla u_h) - f, \alpha \cdot \nabla u_h \\ \qquad\qquad\qquad\qquad\qquad\qquad -\nabla \cdot (D\nabla u_h))_k \ , \\ Q_{USFEM}(u_h, v_h) = \sum_K \tau_k(\alpha \cdot \nabla u_h - \nabla \cdot (D\nabla u_h) - f, \alpha \cdot \nabla u_h \\ \qquad\qquad\qquad\qquad\qquad\qquad +\nabla \cdot (D\nabla u_h))_k \ . \end{cases} \tag{3.11}$$

The stability of the SUPG method for transient convection–diffusion equations is studied in [11]. In the work by Onate [56], it was proven that the stabilization terms can be interpreted as a natural contribution to the governing differential equations of advection–diffusion problems. By considering the concept of flow equilibrium, the stabilization terms emerging in methods such as SUPG, Subgrid Scale (SS), GLS, Lax–Wendroff, Characteristic Galerkin, Laplacian pressure operator etc., are not introduced as correction terms at the discretization level but rather derive naturally. For a comprehensive analysis of SFEM for the stationary or non-stationary advection–diffusion–reaction equation, the review by Codina [19] is recommended.

Writing the advection–diffusion equation in its first-order form via introduction of the flux of the scalar field as an additional unknown is suited for many problems where higher accuracy of the flux is important such a flow in porous media. Masud et al. studied the first-order form of the advection–diffusion equation in the framework of SFEM [54].

Based on the partition of unity framework that is an instance of the Generalized Finite Element Method (GFEM), Turner et al. improved the performance of the Galerkin formulation designing enrichment functions using *a priori* knowledge about the qualitative behavior of solution to make better choices for the local approximation space [65]. The proposed method differs from the standard stabilization strategies as stability is not achieved by adding terms but by multiplying the polynomial with the enrichment functions.

3.2 Test problem for the advection–diffusion equation

In this section we present a test problem for highlighting the capability of FE methods in providing accurate numerical solutions when the Peclet number is substantially large. It was described previously that the solution involves non–physical oscillations in the classical Galerkin method for the case of convective flows with large Peclet number [14]. A square domain, $\Omega = [0,1] \times [0,1]$ is assumed, and the partial differential equation (PDE)introduced in eq. 3.1, the advection–diffusion equation is considered in $\Omega \times [0,T]$, $T \in \mathbb{R}$, with homogeneous boundary conditions $u = 0$ in $\Gamma \times [0,T]$ and initial condition $u = u_0$ on $\Omega \times 0$.

For the initial condition we introduce a characteristic function given by the expression,

$$u_0(\bar{r}) = (1 - 25\text{dist}\,(\bar{r}, [a,a]))\, \mathrm{X}_{\mathrm{B}_{\beta\,(a,a)}},$$

where $\mathrm{X}_{\mathrm{B}_{\beta\,(a,a)}}$ is a function of set X, $\mathrm{B}_{\beta\,(a,a)}$ is a ball of radius β and center (a,a). The $dist\,(\bar{r}_1, \bar{r}_2])$ is the Euclidean distance between points $\bar{r}_1, \bar{r}_2$. In Figure 3.1 we present the initial u distribution for $t = 0$. The computational domain is composed of 2500 Lagrange crossed finite elements with three degrees of freedom, for more details on the finite elements the reader could visit Chapter 2. For the convective field in the advection–diffusion equation, eq. 3.1, we assume a constant field, $\alpha = (0.4, 0.4)$. The total time considered was, $t = 1$, with a time step of, $dt = 0.1$.

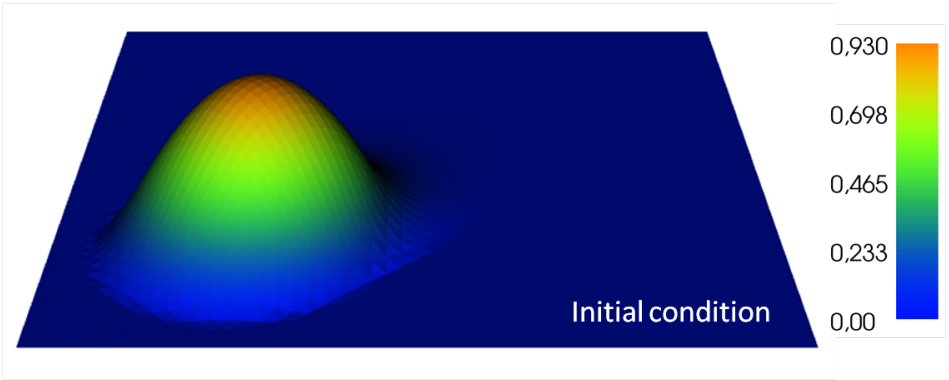

Figure 3.1: Initial u distribution for t = 0.

We apply the three FEMs, described before, the classical Galerkin FE

method, the streamline upwind Petrov–Galerkin (SUPG) method [16], and the Galerkin least squares (GLS) method [37].

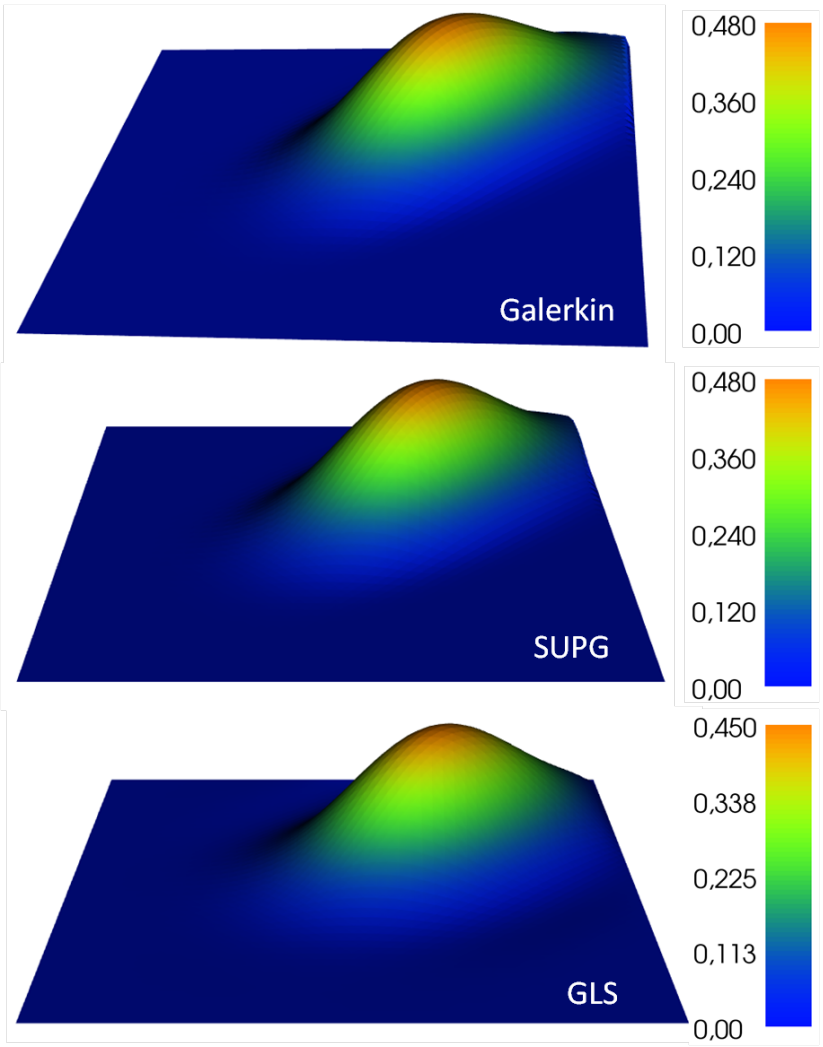

Figure 3.2: Solving the advection–diffusion equation for small Peclet number, $Pe = 10^3$, with three FE methods, the classical Galerkin, the streamline upwind Petrov–Galerkin (SUPG) method, and the Galerkin least squares (GLS).

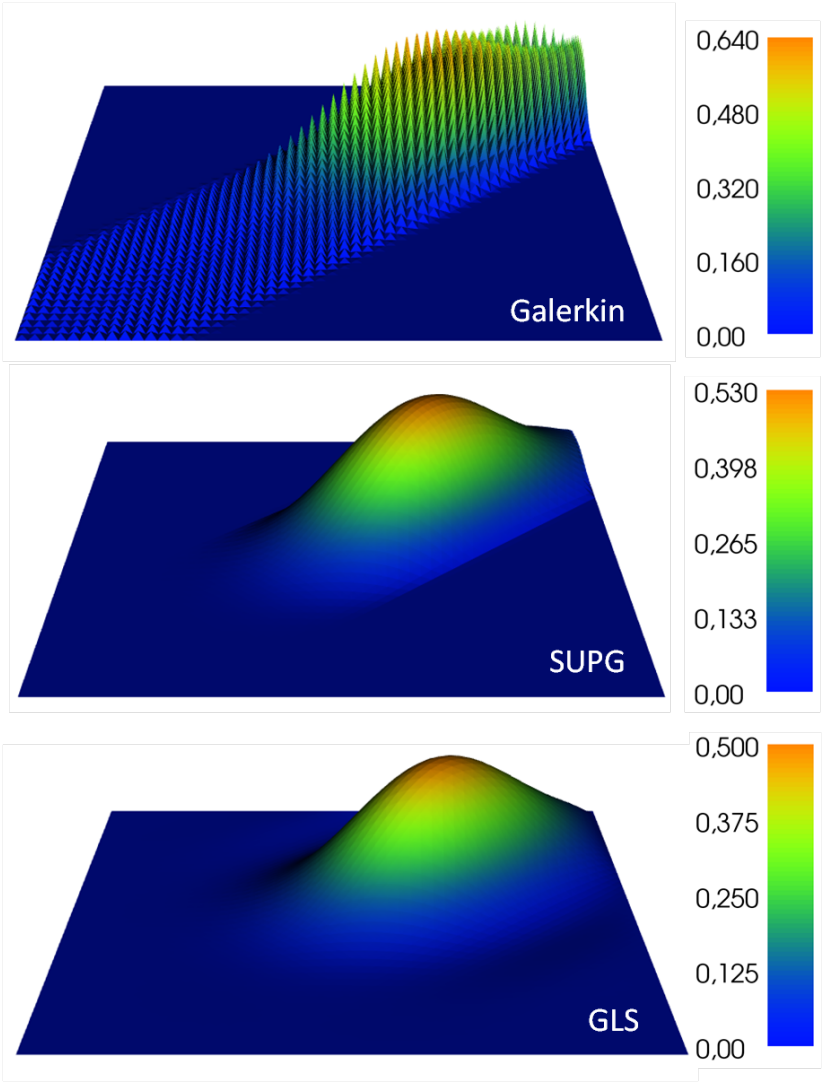

Figure 3.3: Solving the advection–diffusion equation for high Peclet number, $Pe = 10^{15}$, with three FE methods, the classical Galerkin, the streamline upwind Petrov–Galerkin (SUPG) method, and the Galerkin least squares (GLS).

We are using the θ-scheme discretization in time and arbitrary FE discretization in space. In the first case we assume a relative small Peclet number, $Pe = |a|h/D = 10^3$. We observe that all FE methods provide accurate numerical solutions and all of them are very close to each other, as depicted in Figure 3.2. On the other hand, when the Peclet number is much larger

then the classical Galerkin method does not produce a smooth numerical solution and the obtained one involves non–physical oscillations, as depicted in Figure 3.3.

In conclusion, we are interested in the advection–diffusion problems because these problems are frequently treated as the point of departure for the study of the non-linear Navier–Stokes equations, that we will study in the next chapter, Chapter 4. The Peclet number, defined as the ratio of the advection and diffusion rates is a characteristic dimensionless number for such problems. We showed with this study that with a small Peclet number, in the diffusion–dominated regime, the standard Galerkin FE method provides a good approximation of the solution. However, as the Peclet number increases, advection–dominated regime, a stabilized method such as the SUPG and GLS methods, provides much better results restricting non–physical oscillations. In the next Chapter, we will focus our attention on the non-linear Navier–Stokes equations, presenting the most interesting stabilized FE methodologies for solving these equations.

CHAPTER 4

Navier-Stokes Equations

The Navier–Stokes equations, named after Claude–Louis Navier and George Gabriel Stokes, describe the motion of viscous fluids. These non–linear equations arise from applying first principles laws, such as the Newton's second law of motion and are coupled with the conservation of mass or continuity equation. The main difference between the Navier–Stokes and the Euler equations for inviscid flows is that the former equations comprise a dissipative system due to the inclusion of viscous terms (second order spatial derivatives of the velocity field) and are not conservation equations such as Euler equations. They describe a variety of physical problems such as the weather, ocean currents, flow in a pipe, airflow around a wing. The Navier–Stokes equations as mathematical models can also be used for the study of blood flow, the design of power stations, the analysis of pollution, and many more flow related applications.

In finite element formulation and computation of incompressible flows (flows with constant density, ρ) there are two main sources of instabilities associated with the classical Galerkin formulation of the Navier–Stokes problem. One source of instabilities is due to the presence of advection terms leading to spurious oscillations mainly in the velocity field, as discussed in the previous section. The other source of instability is due to an inappropriate combination of interpolation functions for the velocity and pressure field. These instabilities usually appear as oscillations primarily in the pressure field [63]. Below, we present the most interesting FE methodologies for solving the Navier–Stokes problem.

4.1 Streamline–Upwind/Petrov–Galerkin (SUPG)

The most popular stabilized method, the Streamline-Upwind/Petrov-Galerkin (SUPG) formulation, was introduced in 1979 for the incompressible Navier–Stokes equations [35, 7]. By augmenting the Galerkin formulation with residual–based terms, the SUPG formulation addressed the instability of the Galerkin technique for convection dominated flows, leading to a stable method with optimal convergence properties. For compressible flows, the SUPG formulation was initially introduced in 1982 [60], but a more thorough presentation of the method with additional examples was published in [38]. The compressible flow SUPG formulation was initially introduced for conservation variables, and later for primitive variables. For more details on these developments, the interested reader is referred to a recent paper on stabilized methods for compressible flows [7].

The incompressible Navier–Stokes equations are written as,

$$\begin{cases} \dot{\mathbf{v}} + \mathbf{v} \cdot \nabla \mathbf{v} - 2\,\nu\,\nabla \cdot \varepsilon(\mathbf{v}) + \nabla p = \mathbf{f}, \quad in\ \Omega \times [0, \mathrm{T}], \\ div\,\mathbf{v} = 0, \quad in\ \Omega \times [0, \mathrm{T}], \\ \mathbf{v} = \mathbf{g}, \quad on\ \Gamma_{\mathbf{g}} \times [0, \mathrm{T}], \\ \sigma \cdot \mathbf{n} = (2\,\nu\,\nabla^s \mathbf{v} - p\mathbf{I}) \cdot \mathbf{n} = \mathbf{h}, \quad on\,\Gamma_{\mathbf{h}} \times [0, \mathrm{T}], \\ \mathbf{v}(\mathbf{x}, 0) = \mathbf{v}_0(\mathbf{x}), \quad on\ \Omega_0, \end{cases} \tag{4.1}$$

where $\mathbf{v}$ is the velocity vector, p is the kinematic pressure, $\mathbf{f}$ is the body force vector, ν is the kinematic viscosity, $\nabla^s \mathbf{v}$ is the symmetric part of the velocity gradient, $\mathbf{I}$ is the identity tensor, and $\varepsilon(\mathbf{v})$ is the strain rate tensor which is defined as, $\varepsilon(\mathbf{v}) = \frac{1}{2}(\nabla \mathbf{v} + \nabla \mathbf{v}^{\mathrm{T}})$. Eqs. (4.1) represent the momentum and continuity equations, with the Dirichlet and Neumann boundary conditions, and the initial condition, respectively.

The Pressure-Stabilizing/Petrov-Galerkin (PSPG) formulation for the Navier –Stokes equations of incompressible flows in the framework of residual–based methods was introduced in [62, 63]. The interested reader can find more of the method in the previous Chapter, Chapter 3, in Section 3.1.2 , pages 34–36.

This method allowed the use of equal–order interpolation functions for the velocity and pressure variables and assured numerical stability and optimal accuracy. An earlier version of the PSPG formulation for the Stokes problem was introduced in [36]. The SUPG and PSPG stabilizations were combined under a single name, the SUPS stabilization method [6, 7].

4.2 Stabilized FEM and the Variational multiscale method (VMS)

Stabilized and multiscale formulations are among the most fundamental and important methodologies for finite element computations of complex fluid mechanics problems. Tezduyar et al. have proposed certain stabilized formulations with bilinear and linear equal–order–interpolation elements for the computation of dynamic and steady incompressible flows [63]. In their study, the stabilization procedure involves a modified Galerkin/least–squares formulation of the steady–state equations. The results from the considered test problems show that the $Q_1 - Q_1$ element is slightly less dissipative than the $P_1 - P_1$ element. The solutions obtained with these elements are in a good argument with the solutions obtained from others studies [61].

For the Navier–Stokes problem (non–linear PDEs with the appropriate conditions), equations (4.1), the bounded domain Ω is descretized into non–overlap-ping regions Ω^e with boundaries Γ^e, $e = 1, 2, ..., n_{el}$, such that $\Omega = \cup_{e=1}^{n_{el}} \Omega^e$. The union of element interiors and element boundaries are, $\Omega' = \bigcup_{e=1}^{n_{el}} (\text{int})\Omega^e$ and $\Gamma' = \bigcup_{e=1}^{n_{el}} \Gamma^e$, respectively. In Variational multiscale method (VMS) the velocity field is decomposed into the sum of the coarse or resolved scales and the fine or subgrid scales [50, 53],

$$\mathbf{v}(\mathbf{x}, t) = \bar{\mathbf{v}}(\mathbf{x}, t) + \mathbf{v}'(\mathbf{x}, t), \tag{4.2}$$

and the weight function is decomposed in its coarse and the fine scale components indicated as $\bar{\mathbf{w}}(\mathbf{x})$ and $\mathbf{w}'(\mathbf{x})$, respectively,

$$\mathbf{w}(\mathbf{x}) = \bar{\mathbf{w}}(\mathbf{x}) + \mathbf{w}'(\mathbf{x}). \tag{4.3}$$

Remark. The main goal of the VMS method is to solve the fine–scale problem, defined over the sum of element interiors to obtain the fine scale solution. This solution is then substituted in the coarse–scale problem, eliminating the explicit appearance of the fine scales while still modeling their effects. Both coarse and fine scale equations are nonlinear equations due to the convection term, and to solve them a linearization is taking place [53].

The resulting equation is expressed in terms of the coarse scales and for the sake of simplicity the superposed bars are dropped. So, the VMS residual–

based stabilized form for the incompressible Navier–Stokes equations is,

$$\begin{aligned}
&(\mathbf{w}, \delta\mathbf{v}_t) + (\mathbf{w}, \delta\mathbf{v} \cdot \nabla\mathbf{v}^{(i)} + \mathbf{v}^{(i)} \cdot \nabla\delta\mathbf{v}) + \beta(\mathbf{w}, \mathbf{v}^{(i)}\nabla \cdot \delta\mathbf{v} + \delta\mathbf{v}\nabla \cdot \mathbf{v}^{(i)}) \\
&+(\nabla^S\mathbf{w}, 2\nu\,\nabla^S\delta\mathbf{v}) - (\nabla \cdot \mathbf{w}, \delta p) + (q, \nabla \cdot \delta\mathbf{v}) \\
&+(\mathbf{v}^{(i)} \cdot \nabla\mathbf{w} + 2\nu\,\Delta\mathbf{w} + \nabla q + (1-\beta)\mathbf{w}\nabla \cdot \mathbf{v}^{(i)}, \tau\,\mathbf{r}_2) \\
&-(1-\beta)\,(\mathbf{w}, (\tau\,\mathbf{r}_2) \cdot \nabla\mathbf{v}^{(i)}) + \beta((\tau\,\mathbf{r}_2) \cdot \nabla\mathbf{w}, \mathbf{v}^{(i)}),
\end{aligned} \tag{4.4}$$

where the last two lines of the equation correspond to the stabilization terms, $\beta \in [0, 1]$, $\mathbf{r}_2$, is the residual from the linearization of the non–linear fine–scale problem, τ, is the fine–scale variational operator, and Δ is the vector Laplacian operator. A significant contribution of the VMS method is the systematic and consistent derivation of the fine–scale variational operator, τ, termed as the stabilization tensor that possesses the right order in the advective and diffusive limits, and variationally projects the fine–scale solution on the coarse–scale space [53]. The stabilization operator can be defined as [50],

$$\begin{aligned}
\tau = {} & b^e \int b^e d\Omega \\
& \times \left[\begin{array}{l} \int (b^e)^2 \nabla^T \mathbf{v}^{(i)} d\Omega + \int b^e \mathbf{v}^{(i)} \cdot \nabla b^e d\Omega\,\mathbf{I} \\ +\beta \int b^e \mathbf{v}^{(i)} \otimes \nabla b^e d\Omega + \beta \int b^e (\nabla \cdot \mathbf{v}^{(i)})\, d\Omega\,\mathbf{I} \\ +\nu \int |\nabla b^e|^2\, d\Omega\,\mathbf{I} + \nu \int \nabla b^e \otimes \nabla b^e d\Omega \end{array} \right]^{-1},
\end{aligned} \tag{4.5}$$

where, $b^e(\xi)$ is a bubble function over Ω'. More details on the derivation and the obtained form of the VMS residual–based stabilized form and the fine–scale variational operator, τ, for the incompressible Navier–Stokes equations can be found in [50, 53]. Massud and collaborators have further extended the VMS methodology for shear–rate dependent non–Newtonian fluids and incompressible turbulent fluid flows [44, 51, **?**].

4.3 Discontinuous and adaptive Galerkin method

In the last decades, discontinuous Galerkin (DG) methods form a class of numerical methods that combine features of the finite element and the finite volume framework, successfully applied to PDEs from a wide range of applications. An overview to DG method for elliptic problems and research directions can be found in [3, 18].

In order to use the equal order interpolation functions for velocity and pressure, the Navier–Stokes equations can be decoupled to distinct equations

through the split method. The obtained equations are nonlinear hyperbolic, elliptic, and Helmholtz equations, respectively. The hybrid method combines DG and FE methods. Therefore, DG method is concerned to accomplish spatial discretization of the nonlinear hyperbolic equation to avoid using stabilization approaches in FEM. The split methods due to their decoupled schemes, allows choosing equal order basis functions for velocity and pressure [22, 29, 31]. Marchandise and Remacle used an implicit pressure stabilized FEM to solve the Navier–Stokes equations, and DG method was employed to deal with the level–set equation [49]. They calculated the velocity and pressure in the coupled momentum equation together with adding stabilization terms for studying two–phase flows. Pandare and Luo proposed a coupled reconstructed discontinuous Galerkin (rDG) method and continuous Galerkin method for the solution of unsteady incompressible Navier–Stokes equations [57] .

In the paper by Gao et al., the main goal is to take full advantage of DG method and FEM on the basis of a split method [24, 40] to deal with the incompressible Navier–Stokes equations [29]. For the spatial discretization, they treat the nonlinear convection term through DG method, which can guarantee stability, accuracy and also avoid stabilization techniques used in FEM. Lomtev and Karniadakis in their study present a new DG method for simulating compressible viscous flows with shocks on standard unstructured grids [47]. This method is based on a discontinuous Galerkin formulation both for the advective and the diffusive terms. High–order accuracy is achieved by using a recently developed hierarchical spectral basis. This basis is formed by combining Jacobi polynomials of high–order weights written in a new coordinate system. It retains a tensor–product property, and provides accurate numerical quadrature. Their formulation is conservative, and monotonicity is enforced by appropriately lowering the basis order and performing *hp*–refinement around discontinuities [47].

Bassi and Rebay introduce a high–order DG method for the numerical solution of the compressible flows [5]. The method combines two main ideas, the physics of wave propagation, accounted for by means of Riemann problems and accuracy being obtained by high–order polynomial approximations within elements. The method is suited to compute high–order accurate solution of the Navier–Stokes equations on unstructured grids. Klaij et al. in their study present a conservative arbitrary Lagrangian Eulerian (ALE) approach to deal with deforming meshes utilizing DG method for optimal flexibility on the local mesh refinement and adjustment of the polynomial order in each element (*hp*-adaptation) [42]. The numerical method allows for local grid adaptation as well as moving and deforming boundaries. Persson and colleagues intro-

duced a method for computing time–dependent solutions to the compressible Navier–Stokes equations on variable geometries [58]. The transport equations are written as a conservation law for the independent variables in the reference configuration, the complexity introduced by variable geometry is reduced to solving a transformed conservation law in a fixed reference configuration. The spatial discretization is carried out using the DG method on unstructured meshes, while time integration is performed by a Runge–Kutta method. The problem under consideration was altered by adding an equation for the time evolution of the transformation Jacobian to the original conservation law and correcting for the accumulated metric errors. Results are discussed to present the capability of the approach to handle high–order approximations on complex geometries [58].

4.4 Test problems and applications

4.4.1 The backward step test problem

In order to describe the effect of stabilized methods in the equations under consideration, we present a test problem for the solution of Stokes equations. The test problem is called the "backward step" and is a well established problem in fluid mechanics applications. We test two FE methods the Classical Galerkin and the Stabilized FE method. We write the Stokes equations with the continuity, in the strong form, as follows,

$$\begin{cases} -\nabla \cdot (\nabla \mathbf{u} + pI) = f \ \ in \ \ \Omega, \\ \qquad\qquad \nabla \cdot u = 0 \ \ in \ \ \Omega. \end{cases} \tag{4.6}$$

The sign of the pressure has been flipped from the classical definition. This is done in order to have a symmetric, but not positive–definite, system of equations rather than a non–symmetric, but positive–definite, system of equations. A typical set of boundary conditions on the boundary $\partial\Omega = \Gamma_D \cup \Gamma_N$ can be,

$$\begin{aligned} u &= u_0 \ \ on \ \ \Gamma_D, \\ \nabla u \cdot n + p\, n &= g \ \ on \ \ \Gamma_N. \end{aligned}$$

The Stokes equations can be formulated in a mixed variational form, a form where the two variables, the velocity, $\mathbf{u}$ and the pressure, p, are approximated simultaneously, where $(\mathbf{u}, p) \in W$. The space W should be a mixed (product) function space, $W = V \times Q$ such that $u \in V$ and $p \in Q$. The classical

formulation, the Galerkin FEM, can be found in Chapter 2, section 2.2.3, page 28. In this problem, we use first order elements in both velocity and

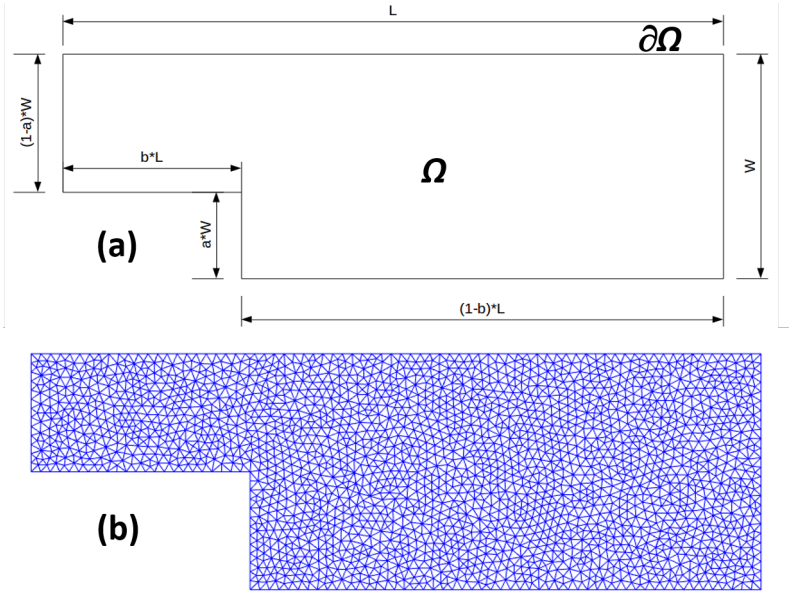

Figure 4.1: (a) The domain Ω and the dimensions of the backward step, (b) the computational mesh composed of approximately 2500 finite elements.

pressure, which will lead to stability problems, spurious solution especially for the pressure field. However, using a stabilized variational formulation we will obtain a smooth solution for both fields, velocity and pressure. Therefore we use a stabilized variational formulation, and we want to find $(\mathbf{u}, p) \in W$, for all $(\mathbf{v}, q) \in W$, such that,

$$a((\mathbf{u}, p), (\mathbf{v}, q)) = L((\mathbf{v}, q)), \tag{4.7}$$

where,

$$\begin{aligned} a\left((\mathbf{u}, p), (\mathbf{v}, q)\right) &= \int_{\Omega} \left(\nabla \mathbf{u} \cdot \nabla \mathbf{v} - \nabla \cdot \mathbf{v} p + \nabla \cdot \mathbf{u} q + \delta \nabla q \cdot \nabla p\right) dx, \\ L\left((\mathbf{v}, q)\right) &= \int_{\Omega} f \cdot \mathbf{v}\, dx + \delta \nabla q \cdot f\, ds, \end{aligned} \tag{4.8}$$

where $\delta = ch^2$, c is a constant and h is the mesh cell size of the computational mesh. The domain Ω and the computational mesh are shown in Figure 4.1,

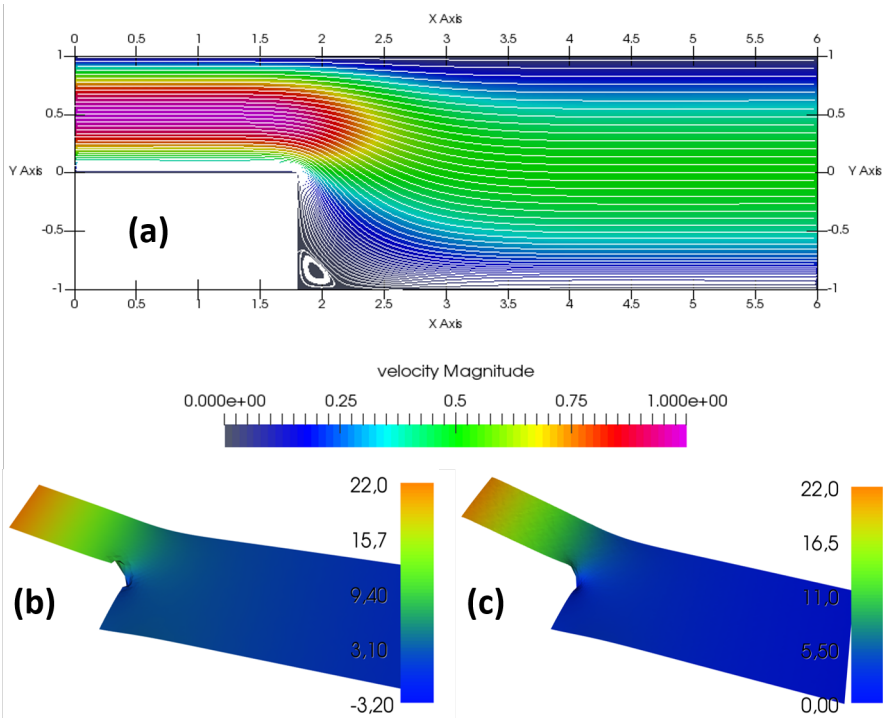

Figure 4.2: (a) Velocity magnitude and streamlines in the domain Ω for the backward step, (b) pressure field for the backward step using the classical Galerkin FEM, (c) pressure field for the backward step using the Stabilized FEM.

where the main dimensions are, $L = 6$, $W = 2$, and the constants are, $a = 0.5$, $b = 0.25$. The computational mesh is composed of approximately 2500 finite elements.

Figure 4.2(a) shows the velocity field in the domain for the backward step. We also present the streamlines in the domain in order to visualize the recirculation close to the step. It is observed that the maximum velocity is in the entrance of the channel and the velocity drops rapidly as the domain expands. In Subfigures 4.2(b) and (c) we visualize the pressure field with the classical Galerkin and Stabilized FEM. It is observed that the pressure field is smooth in Subfigures 4.2(c) even though we use first order elements in both velocity and pressure, which expected to lead to stability problems and spurious solution especially for the pressure field. However, the pressure field for the Stabilized FEM is smoother than in the Galerkin FEM. This test problems highlights

the importance of Stabilized FEM. In the next section we present a Stabilized FEM for the solution of the Navier–Stokes equations in a three–dimensional patient–based domain. The stabilized method (SUPG) is expected to provide smooth solution for both velocity and pressure fields.

4.5 Application in Biomedical Engineering

In this subsection we present the dynamic numerical solution on a three–dimensional patient–based carotid artery reconstructed from computed tomography angiography (CTA) data. The data set of the CTA images were taken in Larissa University Hospital or in Euromedica Medical Diagnostic Center of Larissa.

4.5.1 Reconstruction of the carotid artery

The three–dimensional model of the carotid artery, including the three main components, the common carotid artery (CCA), the internal carotid artery (ICA) and the external carotid artery (ECA), was constructed using the CTA data of a treated patient. The reconstruction of the DICOM images into a three-dimensional model that preserves the geometry of the lumen postoperatively, was performed in the image processing and reconstruction open source software, ITK–SNAP. Then, the model was smoothed with Materialise Mimics (Materialise, Leuven, Belgium). The reconstructed geometry of the carotid artery was subsequently meshed with tetrahedral elements.

4.5.2 Mathematical Formulation and boundary conditions

There is a strong correlation between atherosclerosis and shear stress. In vitro studies concerning hemodynamic in adult carotid bifurcations have shown that regions of atherosclerotic plaque formation and maximum intimal thickening were related with low and oscillatory shear stress values, while the marginally affected arterial lesions were exposed to high shear stress and high flow velocities [43]. This suggests that low shear stress may promote atherogenesis in the carotid bifurcation.

The equations describing the flow in the carotid artery are the Navier–Stokes equations described in the previous sections (**see above sections,**

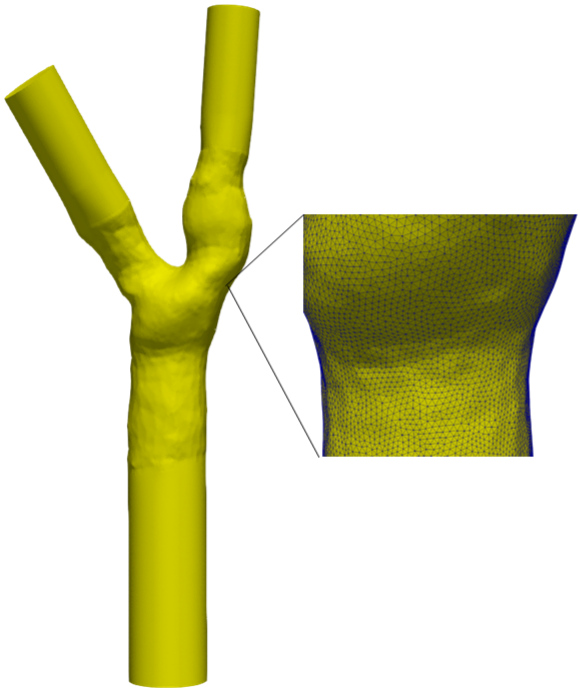

Figure 4.3: The three–dimensional carotid bifurcation of the geometry under consideration.

Streamline–Upwind/Petrov–Galerkin (SUPG) and Variational multiscale method (VMS) & stabilized FEM). We solve numerically these equations with appropriate boundary conditions. Concerning boundary conditions applied in the three–dimensional patient–based carotid geometry, we follow the study by Hoi et al. 2010, and apply the corresponding dynamic flow rates at the entrance of the CCA and at the exit of ICA [34]. Furthermore, a resistance boundary condition was applied at ECA, describing the resistance of blood to flow due to the downstream vasculature.

4.5.3 Sensitivity Analysis

Different meshes have been created with different elements dimensions. All meshes are radial with tetrahedral elements. Steady state simulations have been performed for each computational mesh with the sensitivity analysis

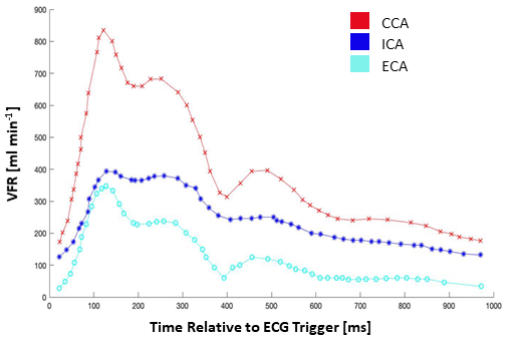

Figure 4.4: The waveforms at the CCA, ICA and ECA as adopted by Hoi et al. 2010 [34].

Table 4.1: Sensitivity analysis, comparison between finest and coarse grids, % difference of average WSS magnitude.

Grid size	WSS % difference
1.431 *mil.*	—
0.488 *mil.*	8.8
0.204 *mil.*	13.0
0.121 *mil.*	16.6

or grid independence study presented in Table 4.1 and using the boundary conditions discussed in the previous subsection.

The results of each simulation were referred to those obtained with the finest mesh (1.431 million elements) and the percentage differences have been calculated for averaged wall shear stress (WSS) of the studied carotid artery.

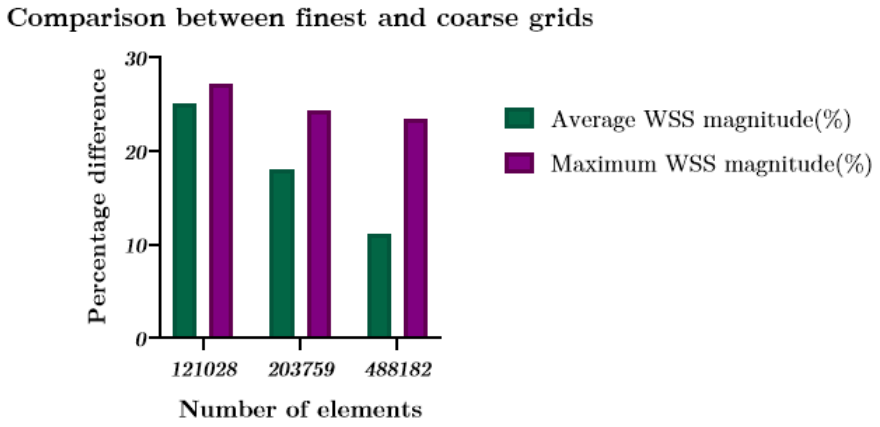

Figure 4.5: Comparison between finest and coarse grids.

4.5.4 FEM unsteady simulations

Blood was considered as a Newtonian fluid. The physical properties of blood, being imposed for the unsteady simulations as well as for the sensitivity analysis, are blood density $\rho = 1050\ kg/m^3$ and viscosity $\mu = 0.0035\ Pa\,s$. The flow was considered laminar during the entire cardiac cycle.

At the inflow section and at the ICA section it was imposed a time velocity profile, according to the flow rate described by Hoi et al. 2010 [34], scaling the velocity in accordance to the boundary area. The mathematical expression for the velocity waveforms was obtained by interpolating samples given by Hoi et al. 2010 [34] with the help of the Fourier series.

The governing partial differential equations of blood flow are discretized with the SUPG method. The resulting coupled system of algebraic equations is solved iteratively and convergence was achieved when residual error of each equation was equal to 10^{-4}. The cardiac cycle was considered to last $1s$, with a fixed time step of $\Delta t = 0.03s$. The simulations were performed for three cardiac cycles in two Intel Xeon processors (E5645, 2.40GHz, 12MB Cache, 5.86GT/s Intel QPI) of a $Dell^{TM}$ $Precision^{TM}$ T7500 workstation). We exclusively utilized the results of the third cardiac cycle avoiding any dynamic disturbances of the numerical solution in the initial cycles.

4.6 Results and discussion

Main findings and results. The numerical results from the simulations are summarized in the Figures 4.6 and 4.7. In these figures, we present the velocity and pressure fields in four different time instances during the entire cardiac cycle. Three instances during the systolic phase and one at the diastolic phase of the cycle revealing the fields under consideration for the patient–based carotid artery. In the figures, above the field, we also highlight the point of the cardiac cycle where the results were taken.

One can see that the highest values of the velocity field are in the CCA and in the narrowest part of the ICA during the entire cardiac cycle. At the beginning of the cardiac cycle, as the flow is accelerating, the velocity gradually increases in the domain, as depicted in Fig. 4.6, subfigures 1 and 2. At the deceleration phase, Fig. 4.6, subfigure 3, we observe that the velocity starts gradually to decrease. Finally, at the last subfigure (subfigure 4), we observe that during the diastolic phase the velocity takes small values and the velocity field seems very disturbed, with several recirculation areas, as expected [66].

In such numerical cases where the pressure field plays important role, advanced numerical approaches should be used. In this thesis, in order to capture as accurate as possible the pressure field, we studied and implemented advanced numerical FE approaches, such as the SUPG FE method. It is imperative to accurate capture the pressure field with smoothed areas of possible discontinuities. To this extend, for the pressure results in the first two time instances, Fig. 4.7, subfigures 1 and 2, in the start of the systolic phase, we have higher pressure values in the entrance of the carotid artery (CCA) compared to the two exits at the smaller arteries (ICA and ECA) after the bifurcation, showing that the flow is strongly forward and the pressure drop is leading the flow. At the other two time instances, Fig. 4.7, subfigures 3 and 4, at the deceleration of the systole and during the diastole, the pressure drop is reversed. These results show that the fluid (blood) continually looses momentum, and decelerates, until diastolic phase where has a small velocity with recirculating areas and very small pressure drop as also revealed in other studies [66].

Discussion and future steps. Through the above analysis one can see that FEM is a very useful numerical method for solving non–linear PDE's in fluid mechani. Other numerical methods are dealing with the governing differential equation where the FEM is dealing with the weak formulation. The SUPG advancements can be very useful as it has been shown that handle effectively the pressure field compared to the classical FE method. The stabilized methods

are also more versatile in terms of complex and non–linear problems.

The obtained results are realistic and can be compared with measurements taken form advanced imaging modalities, such as ultrasound, showing good agreement. The presented results have several advancements beyond the numerical approach used, the SUPG method. Other advancements of the study are the altered boundary conditions we applied to solve the problem under consideration and the fact that the structure we used is a patient–based geometry reconstructed from CTA data. This geometry represents in detail the actual patient's geometry. Additionally, we performed advanced time dependent large scale simulations that require parallel processing of the computational grids. All these advancements show the difficulty to solve such problems and provide accurate and realistic results. Due to the development of the numerical methods in the last decades, we have the capability to numerically solve very difficult and non–linear problems such the one presented here.

As future steps, we could propose to develop this methodology as a reliable workflow for the carotid arteries and other biomedical applications. The evaluation of several important indices could also be an interesting next step. Such indices are the time averaged wall shear stress (TAWSS), the oscillatory shear index (OSI) and the relative resistance time (RRT) that provide information about the thrombogenic potential of the geometry under consideration.

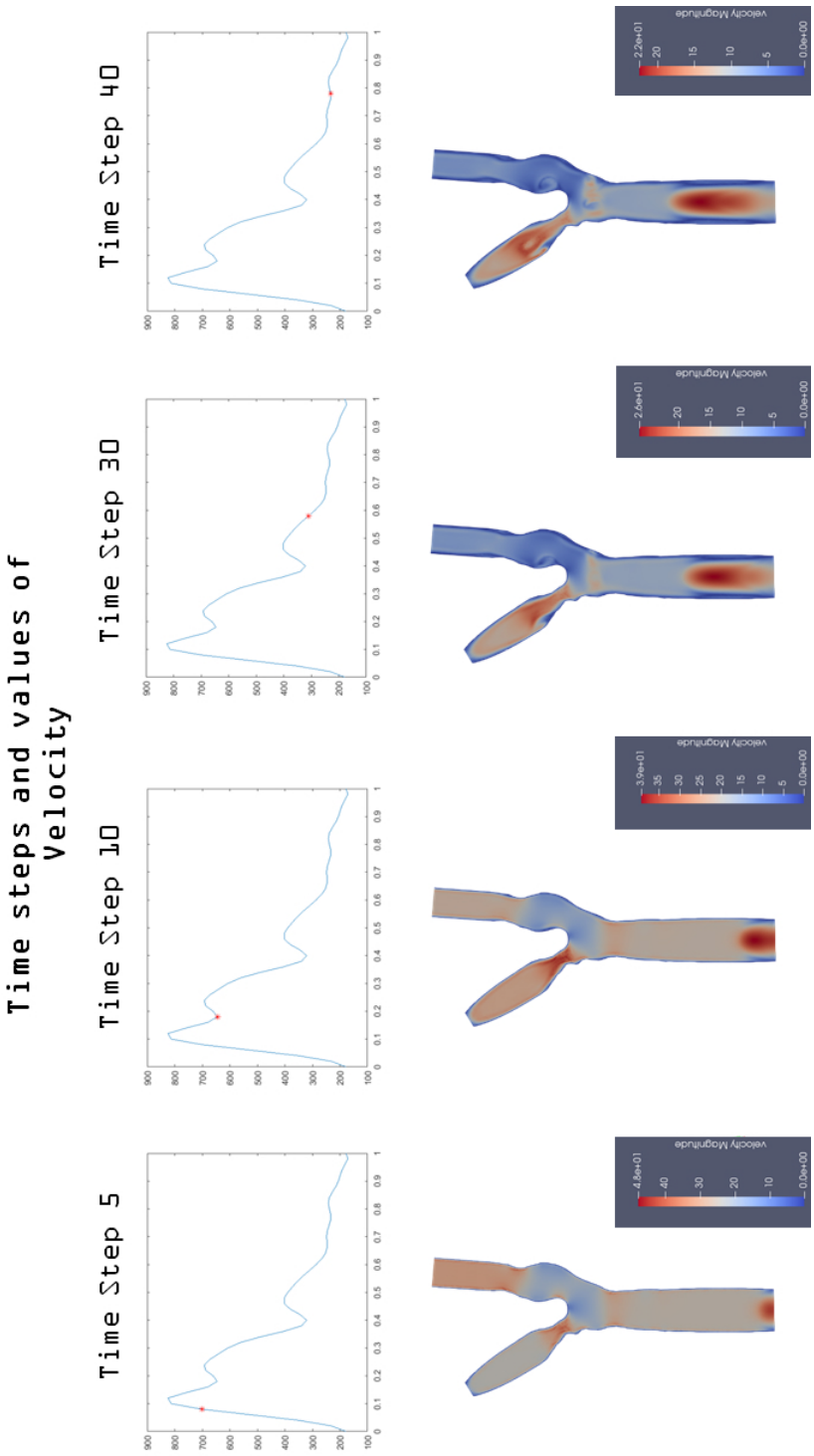

Figure 4.6: Velocity Results

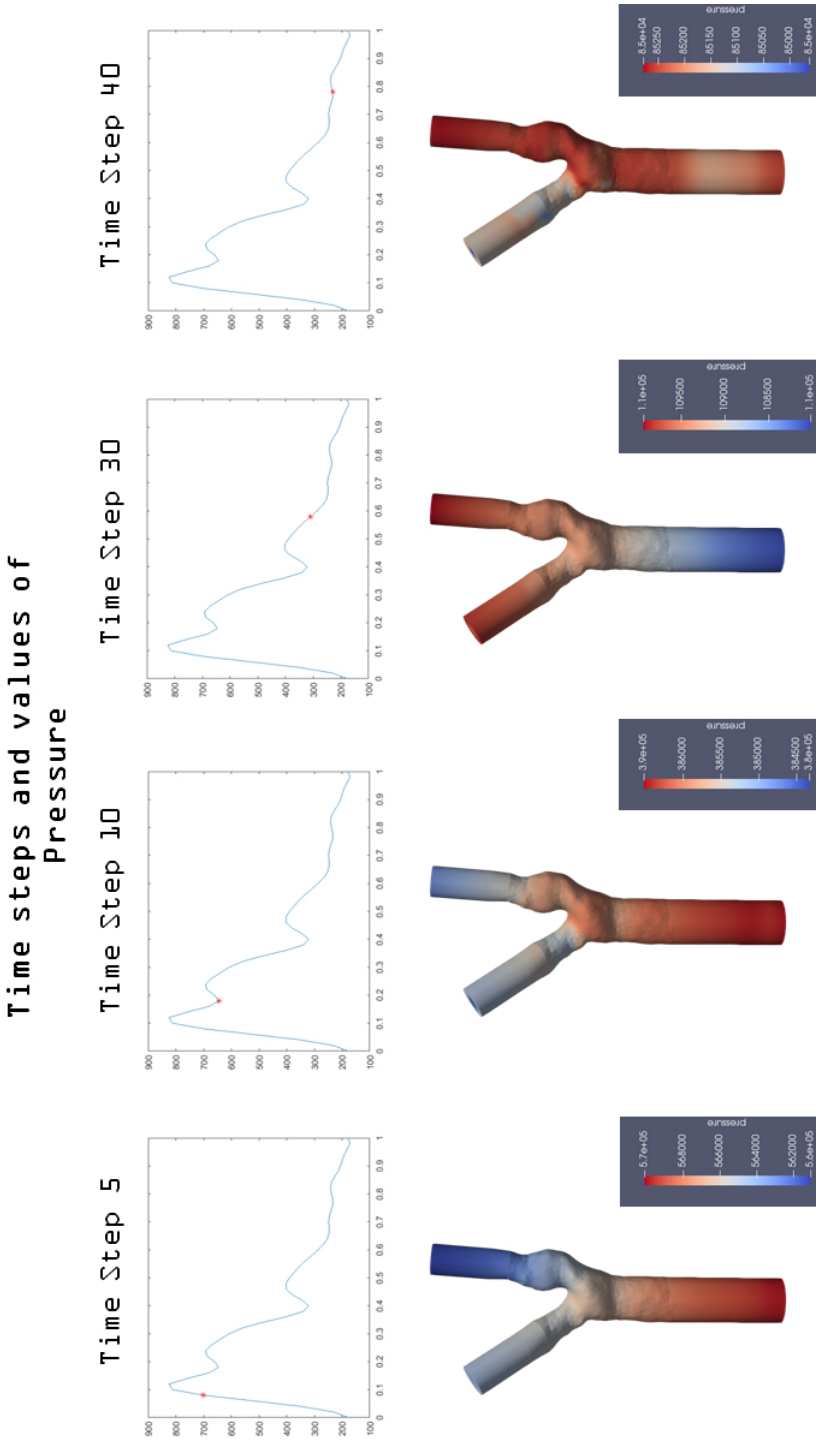

Figure 4.7: Pressure Results

CHAPTER 5

Conclusions

Summarizing, in this thesis we analyzed the Finite Element Method, initially in a theoretical basis, presenting the most relevant theorems for existence and uniqueness of the numerical solution of boundary value problems of PDE systems. Main aim of this study is to apply the FEM in Fluid Mechanics problems that are difficult or impossible to be solved analytically.

We further introduced *a priori* and *a posteriori* error estimates for linear boundary value problems, such as the Stokes problem that is a well studied problem of the literature. However, we are lacking these estimates for non-linear problems, such as the Navier–Stokes problems. We present the notion of the shape function used in FEM method and discussed several types of such function and the various elements that can be used in FEM.

Before studying the more complex and non–linear problem, we focus on the numerical solution of the advection–diffusion equation, this is a scalar PDE that has many difficulties due to the advection terms. So, in the last decades, there are several advancements for the solution of this equation. One of these advancements is the stabilized or upwind method known as the SUPG method. Other presented methodologies are the least squares FEM (GLS)and the unusual stabilized FEM (USFEM).

The last chapter is dedicated to the numerical solution of the Navier–Stokes (N–S) problem. At the beginning we present the strong formulation of the N–S problem and the weak formulation for several advanced FE methods, which can handle the non-linear problem for large Reynolds numbers. More precisely we present the SUPG, variational multiscale method (VMS) and briefly the discontinuous Galerkin.

We present a group of well established test problems, such as the driven cavity and the backward step, to show that these FE methodologies provide reliable numerical solutions for a wide range of Peclet and Reynolds numbers.

Finally, we focus on a biomedical application, developing a 3D patient–based mathematical model of a carotid artery. The results show that the SUPG FEM can be used to describe the numerical solution in such 3D dynamical problems with extensions from mathematics to the biomedical field.

Appendix A

Miscellaneous Mathematical Concepts

Banach Space A normed linear space $(V, \|\cdot\|)$ which is complete with respect to the metric induced by the norm, $\|\cdot\|$.

Bilinear Form A bilinear form, $b(\cdot,\cdot)$, on a linear space V is a mapping $b : V \times V \longrightarrow \mathcal{R}$ such that each of the maps $v \mapsto b(v,w)$ and $w \mapsto b(v,w)$ is a linear form on V.

Symmetric The bilinear form is symmetric if $b(v,w) = b(w,v)$, for all $v, w \in V$.

Boundary Conditions Are constraints necessary for the solution of a differential equation (or system of differential equations), known as boundary value problem, in a domain.

Dirichlet This condition specifies the value that the unknown function needs to take on along the boundary of the domain.

Neumann This condition specifies the values that the derivative of a solution is going to take on the boundary of the domain.

Hilbert Space Let $(V, (\cdot,\cdot))$ be an inner-product space. If it is complete then $(V, (\cdot,\cdot))$ is called Hilbert space.

Strong Form Is the initial form of the equation.

Sobolev Space Is a vector space of functions equipped with a norm that is a combination of L^p-norms of the function itself and its derivatives up to a given order. We define the Soboleve spaces via

$$W_p^k(\Omega) := \left\{ f \in L_?^1(\Omega) : \|f\|_{W_p^k(\Omega)} < \infty \right\}$$

In the cases where $p = 2$ Sobolev spaces are a form of a Hilbert space.

Inner Product A inner product on a linear space V satisfies the following

(a) $(u + v, w) = (u, w) + (v, w)$
(b) $(cu, v) = c(u, v),\ c \in \mathbb{R}$
(c) $(v, v) \geq 0,\ \forall v \in V$ and
(d) $(v, v) = 0 \iff v = 0$.

Norm Given a linear (vector)space V, a norm, $\|\cdot\|$, is a function on V with valuesnin the non-negative reals having the following properties:

(a) $\|v\| \geq 0\ \forall v \in V$ and
$\|v\| = 0 \iff v = 0$
(b) $\|c \cdot v\| = |c| \cdot \|v\|\ \ \forall c \in \mathcal{R}, v \in V$, and
(c) $\|v + w\| \leq \|v\| + \|w\|\ \ \forall v, w \in V$
(triangular inequality).

Appendix B

Acronyms

Acronyms

ALE	Arbitrary Lagrangian Eulerian
CBS	Characteristic Base Split
CCA	Common Carotid Artery
CTA	Computed Tomography Angiography
DG	Discontinuous Galerkin
DICOM	Digital Imaging and Communications in Medicine, (file type)
ECA	External Carotid Artery
FEA	Finite Element Analysis
FEM	Finite Element Method
GLS	Galerkin Least Squares
GSM	Gradient Smoothed Method
ICA	Internal Carotid Artery

LBB	Ladyzhenskaya–Brezzi–Babuska
ODE	Ordinary Differential Equation
PDE	Partial Differential Equation
RTN	Raviart-Thomas-Nedelec
SUPG	Streamline Upwind Petrov–Galerkin
VMS	Variational Multiscale Scheme
WRM	Weighted Residual Method
WSS	Wall Shear Stress

Bibliography

[1] Akrivis, G., Crouzeix, M., and Makridakis, C. Implicit-explicit multistep methods for quasilinear parabolic equations. *Numerische Mathematik 82*, 4 (1999), 521–541.

[2] Argyris, J. H., and Kelsey, S. *Energy theorems and structural analysis*, vol. 960. Springer, 1960.

[3] Arnold, D. N., Brezzi, F., Cockburn, B., and Marini, L. D. Unified analysis of discontinuous galerkin methods for elliptic problems. *SIAM Journal on Numerical Analysis 39*, 5 (2002), 1749–1779.

[4] Arnold, D. N., Brezzi, F., and Fortin, M. A stable finite element for the stokes equations. *Calcolo 21*, 4 (1984), 337–344.

[5] Bassi, F., and Rebay, S. A high-order accurate discontinuous finite element method for the numerical solution of the compressible navier–stokes equations. *Journal of Computational Physics 131*, 2 (1997), 267–279.

[6] Bazilevs, Y., Takizawa, K., and Tezduyar, T. E. *Computational fluid-structure interaction: methods and applications*. John Wiley & Sons, 2013.

[7] Bazilevs, Y., Takizawa, K., and Tezduyar, T. E. New directions and challenging computations in fluid dynamics modeling with stabilized and multiscale methods. *Mathematical Models and Methods in Applied Sciences 25*, 12 (2015), 2217–2226.

[8] Bercovier, M., and Pironneau, O. Error estimates for finite element method solution of the stokes problem in the primitive variables. *Numerische Mathematik 33*, 2 (Jun 1979), 211–224.

[9] Bergam, A., Bernardi, C., and Mghazli, Z. A posteriori analysis of the finite element discretization of some parabolic equations. *Mathematics of Computation 74*, 251 (2005), 1117–1138.

[10] Bernardi, C., and Verfürth, R. A posteriori error analysis of the fully discretized time-dependent stokes equations. *ESAIM: Mathematical Modelling and Numerical Analysis 38*, 3 (2004), 437–455.

[11] Bochev, P. B., Gunzburger, M. D., and Shadid, J. N. Stability of the supg finite element method for transient advection–diffusion problems. *Computer Methods in Applied Mechanics and Engineering 193*, 23-26 (2004), 2301–2323.

[12] Borker, R., Farhat, C., and Tezaur, R. A discontinuous galerkin method with lagrange multipliers for spatially-dependent advection-diffusion problems. *Computer Methods in Applied Mechanics and Engineering 327* (2017), 93–117.

[13] Brenner, S., and Scott, R. *The mathematical theory of finite element methods*, vol. 15. Springer Science & Business Media, 2007.

[14] Brezzi, F., Bristeau, M.-O., Franca, L. P., Mallet, M., and Roge, G. A relationship between stabilized finite element methods and the galerkin method with bubble functions. *Computer Methods in Applied Mechanics and Engineering 96*, 1 (1992), 117–129.

[15] Brezzi, F., and Fortin, M. *Mixed and hybrid finite element methods*, vol. 15. Springer Science & Business Media, 2012.

[16] Brooks, A. N., and Hughes, T. J. Streamline upwind/petrov–galerkin formulations for convection dominated flows with particular emphasis on the incompressible navier–stokes equations. *Computer Methods in Applied Mechanics and Engineering 32*, 1-3 (1982), 199–259.

[17] Chatzipantelidis, P., Lazarov, R., and Thomée, V. Error estimates for a finite volume element method for parabolic equations in convex polygonal domains. *Numerical Methods for Partial Differential Equations 20*, 5 (2004), 650–674.

[18] Cockburn, B., Karniadakis, G. E., and Shu, C.-W., Eds. *Discontinuous Galerkin Methods*. Springer Berlin Heidelberg, 2000.

[19] Codina, R. Comparison of some finite element methods for solving the diffusion-convection-reaction equation. *Computer Methods in Applied Mechanics and Engineering 156*, 1-4 (1998), 185–210.

[20] Crouzeix, M., and Raviart, P.-A. Conforming and nonconforming finite element methods for solving the stationary stokes equations i. *Revue Française d'Aautomatique Informatique Recherche Opérationnelle. Mathématique 7*, R3 (1973), 33–75.

[21] Dawson, C., and Kirby, R. Solution of parabolic equations by backward euler-mixed finite element methods on a dynamically changing mesh. *SIAM Journal on Numerical Analysis 37*, 2 (1999), 423–442.

[22] Deville, M. O., Fischer, P. F., and Mund, E. H. *High-order methods for incompressible fluid flow*, vol. 9. Cambridge University Press, 2002.

[23] Eriksson, K., and Johnson, C. Adaptive finite element methods for parabolic problems i: A linear model problem. *SIAM Journal on Numerical Analysis 28*, 1 (1991), 43–77.

[24] Ferrer, E., and Willden, R. A high order discontinuous galerkin finite element solver for the incompressible Navier–Stokes equations. *Computers & Fluids 46*, 1 (2011), 224–230.

[25] Fletcher, C. *Computational techniques for fluid dynamics I*. Springer-Verlag, 1988.

[26] Fletcher, C. *Computational techniques for fluid dynamics II*. Springer-Verlag, 1988.

[27] Franca, L. P., and Farhat, C. Bubble functions prompt unusual stabilized finite element methods. *Computer Methods in Applied Mechanics and Engineering 123*, 1-4 (1995), 299–308.

[28] Franca, L. P., Hauke, G., and Masud, A. Revisiting stabilized finite element methods for the advective-diffusive equation. *Computer Methods in Applied Mechanics and Engineering 195*, 13-16 (6 2006), 1560–1572.

[29] Gao, P., Ouyang, J., Dai, P., and Zhou, W. A coupled continuous and discontinuous finite element method for the incompressible flows. *International Journal for Numerical Methods in Fluids 84*, 8 (2017), 477–493.

[30] Ghia, U., Ghia, K. N., and Shin, C. High-re solutions for incompressible flow using the navier-stokes equations and a multigrid method. *Journal of Computational Physics 48*, 3 (1982), 387–411.

[31] Guermond, J.-L., Minev, P., and Shen, J. An overview of projection methods for incompressible flows. *Computer Methods in Applied Mechanics and Engineering 195*, 44-47 (2006), 6011–6045.

[32] Heinrich, J., Huyakorn, P., Zienkiewicz, O., and Mitchell, A. An "upwind" finite element scheme for two-dimensional convective transport equation. *International Journal for Numerical Methods in Engineering 11*, 1 (1977), 131–143.

[33] Heywood, J. G., and Rannacher, R. Finite element approximation of the nonstationary Navier–Stokes problem. i. regularity of solutions and second-order error estimates for spatial discretization. *SIAM Journal on Numerical Analysis 19*, 2 (1982), 275–311.

[34] Hoi, Y., Wasserman, B. A., Xie, Y. J., Najjar, S. S., Ferruci, L., Lakatta, E. G., Gerstenblith, G., and Steinman, D. A. Characterization of volumetric flow rate waveforms at the carotid bifurcations of older adults. *Physiological Measurement 31*, 3 (2010), 291.

[35] Hughes, T., and Brooks, A. A multidimensional upwind scheme with no crosswind diffusion, in, tjr hughes, ed. *Finite Element Methods for Convection Dominated Flows*, 19–35.

[36] Hughes, T. J., Franca, L. P., and Balestra, M. A new finite element formulation for computational fluid dynamics: V. circumventing the babuška-brezzi condition: A stable petrov-galerkin formulation of the stokes problem accommodating equal-order interpolations. *Computer Methods in Applied Mechanics and Engineering 59*, 1 (1986), 85–99.

[37] Hughes, T. J., Franca, L. P., and Hulbert, G. M. A new finite element formulation for computational fluid dynamics: Viii. the galerkin/least-squares method for advective-diffusive equations. *Computer Methods in Applied Mechanics and Engineering 73*, 2 (1989), 173–189.

[38] Hughes, T. J., and Tezduyar, T. Finite element methods for first-order hyperbolic systems with particular emphasis on the compressible euler equations. *Computer methods in applied mechanics and engineering 45*, 1-3 (1984), 217–284.

[39] Karakatsani, F., and Makridakis, C. A posteriori estimates for approximations of time-dependent stokes equations. *IMA Journal of numerical analysis 27*, 4 (2006), 741–764.

[40] Karniadakis, G. E., Israeli, M., and Orszag, S. A. High-order splitting methods for the incompressible navier-stokes equations. *Journal of computational physics 97*, 2 (1991), 414–443.

[41] Kemmochi, T. On the finite element approximation for non-stationary saddle-point problems. *Japan Journal of Industrial and Applied Mathematics* (2017), 1–17.

[42] Klaij, C. M., van der Vegt, J. J., and van der Ven, H. Space–time discontinuous galerkin method for the compressible Navier–Stokes equations. *Journal of Computational Physics 217*, 2 (2006), 589–611.

[43] Ku, D. N., Giddens, D. P., Zarins, C. K., and Glagov, S. Pulsatile flow and atherosclerosis in the human carotid bifurcation. positive correlation between plaque location and low oscillating shear stress. *Arteriosclerosis: An Official Journal of the American Heart Association, Inc. 5*, 3 (1985), 293–302.

[44] Kwack, J., and Masud, A. A stabilized mixed finite element method for shear-rate dependent non-newtonian fluids: 3d benchmark problems and application to blood flow in bifurcating arteries. *Computational Mechanics 53*, 4 (2014), 751–776.

[45] Lakkis, O., and Makridakis, C. Elliptic reconstruction and a posteriori error estimates for fully discrete linear parabolic problems. *Mathematics of computation 75*, 256 (2006), 1627–1658.

[46] Larson, M. G., and Målqvist, A. A posteriori error estimates for mixed finite element approximations of parabolic problems. *Numerische Mathematik 118*, 1 (2011), 33–48.

[47] Lomtev, I., and Karniadakis, G. E. A discontinuous galerkin method for the Navier–Stokes equations. *International journal for numerical methods in fluids 29*, 5 (1999), 587–603.

[48] Makridakis, C., and Nochetto, R. H. Elliptic reconstruction and a posteriori error estimates for parabolic problems. *SIAM journal on numerical analysis 41*, 4 (2003), 1585–1594.

[49] Marchandise, E., and Remacle, J.-F. A stabilized finite element method using a discontinuous level set approach for solving two phase incompressible flows. *Journal of computational physics 219*, 2 (2006), 780–800.

[50] Masud, A., and Calderer, R. A variational multiscale stabilized formulation for the incompressible Navier–Stokes equations. *Computational Mechanics 44*, 2 (2009), 145–160.

[51] Masud, A., and Calderer, R. A variational multiscale method for incompressible turbulent flows: Bubble functions and fine scale fields. *Computer Methods in Applied Mechanics and Engineering 200*, 33-36 (2011), 2577–2593.

[52] Masud, A., and Khurram, R. A multiscale/stabilized finite element method for the advection-diffusion equation. *Computer Methods in Applied Mechanics and Engineering 193*, 21-22 (4 2004), 1997–2018.

[53] Masud, A., and Khurram, R. A multiscale finite element method for the incompressible Navier–Stokes equations. *Computer Methods in Applied Mechanics and Engineering 195*, 13-16 (2006), 1750–1777.

[54] Masud, A., and Kwack, J. A stabilized mixed finite element method for the first-order form of advection–diffusion equation. *International journal for numerical methods in fluids 57*, 9 (2008), 1321–1348.

[55] Nochetto, R. H., Siebert, K. G., and Veeser, A. Theory of adaptive finite element methods: an introduction. In *Multiscale, nonlinear and adaptive approximation*. Springer, 2009, pp. 409–542.

[56] Onate, E. Derivation of stabilized equations for numerical solution of advective-diffusive transport and fluid flow problems. *Computer Methods in Applied Mechanics and Engineering 151*, 1-2 (1998), 233–265.

[57] Pandare, A. K., and Luo, H. A hybrid reconstructed discontinuous galerkin and continuous galerkin finite element method for incompressible flows on unstructured grids. *Journal of Computational Physics 322* (2016), 491–510.

[58] Persson, P.-O., Bonet, J., and Peraire, J. Discontinuous galerkin solution of the Navier–Stokes equations on deformable domains. *Computer Methods in Applied Mechanics and Engineering 198*, 17-20 (2009), 1585–1595.

[59] Tenek, L. T., and Argyris, J. *Finite element analysis for composite structures*, vol. 59. Springer Science & Business Media, 2013.

[60] Tezduyar, T., and Hughes, T. Development of time-accurate finite element techniques for first-order hyperbolic systems with particular emphasis on the compressible euler equations. *NASA Technical Report NASA-CR-204772, NASA* (1982).

[61] Tezduyar, T., Mittal, S., and Shih, R. Time-accurate incompressible flow computations with quadrilateral velocity-pressure elements. *Computer Methods in Applied Mechanics and Engineering 87*, 2-3 (1991), 363–384.

[62] Tezduyar, T. E. Stabilized finite element formulations for incompressible flow computations. In *Advances in applied mechanics*, vol. 28. Elsevier, 1991, pp. 1–44.

[63] Tezduyar, T. E., Mittal, S., Ray, S., and Shih, R. Incompressible flow computations with stabilized bilinear and linear equal-order-interpolation velocity-pressure elements. *Computer Methods in Applied Mechanics and Engineering 95*, 2 (1992), 221–242.

[64] Thomée, V. *Galerkin Finite Element Methods for Parabolic Problems.* Springer-Verlag New York, Inc., 2006.

[65] Turner, D., Nakshatrala, K., and Hjelmstad, K. A stabilized formulation for the advection–diffusion equation using the generalized finite element method. *International Journal for Numerical Methods in Fluids 66*, 1 (2011), 64–81.

[66] Xenos, M. An euler–lagrange approach for studying blood flow in an aneurysmal geometry. *Proceedings of the Royal Society A: Mathematical, Physical and Engineering Sciences 473*, 2199 (2017), 20160774.

[67] Zlámal, M. A finite element procedure of the second order of accuracy. *Numerische Mathematik 14*, 4 (1970), 394–402.